The tectonic and metallogenic framework of Myanmar: A Tethyan mineral system

Nicholas J. Gardiner, Laurence J. Robb, Christopher K. Morley, Michael P. Searle, Peter A. Cawood, Martin J. Whitehouse, Christopher L. Kirkland, Nick M.W. Roberts, Tin Aung Myint

PII: S0169-1368(16)30105-6
DOI: doi: 10.1016/j.oregeorev.2016.04.024
Reference: OREGEO 1799

To appear in: *Ore Geology Reviews*

Received date: 2 March 2016
Revised date: 23 April 2016
Accepted date: 27 April 2016

Please cite this article as: Gardiner, Nicholas J., Robb, Laurence J., Morley, Christopher K., Searle, Michael P., Cawood, Peter A., Whitehouse, Martin J., Kirkland, Christopher L., Roberts, Nick M.W., Myint, Tin Aung, The tectonic and metallogenic framework of Myanmar: A Tethyan mineral system, *Ore Geology Reviews* (2016), doi: 10.1016/j.oregeorev.2016.04.024

The Tectonic and Metallogenic Framework of Myanmar: A Tethyan Mineral System

Nicholas J. Gardiner[1,9*], Laurence J. Robb[1], Christopher K. Morley[2,3], Michael P. Searle[1], Peter A. Cawood[4], Martin J. Whitehouse[5], Christopher L. Kirkland[6], Nick M.W. Roberts[7], Tin Aung Myint[8]

1. Department of Earth Sciences, University of Oxford, Oxford OX1 3AN, United Kingdom.

2. Department of Geological Sciences, Chiang Mai University, Thailand.

3. PPT Exploration and Production, Vibhavadi-Rangsit Road, soi 11, Bangkok, Thailand 10900.

4. Department of Earth Sciences, University of St Andrews, North Street, St Andrews KY16 9AL, United Kingdom

5. Swedish Museum of Natural History, and Nordic Center for Earth Evolution, Box 50007, SE-104 05 Stockholm, Sweden.

6. Centre for Exploration Targeting – Curtin Node, Department of Applied Geology, Western Australian School of Mines, Curtin University, Perth, WA 6845, Australia.

7. NERC Isotope Geosciences Laboratory, British Geological Survey, Keyworth, Nottingham NG12 5GG, United Kingdom.

8. Department of Geology, Mandalay University, Mandalay, Myanmar.

9. Presently at: Centre for Exploration Targeting – Curtin Node, Department of Applied Geology, Western Australian School of Mines, Curtin University, Perth, WA 6845, Australia.

*Corresponding author. E-mail address: nicholas.gardiner@curtin.edu.au

Abstract

Myanmar is perhaps one of the World's most prospective but least explored minerals jurisdictions, containing important known deposits of tin, tungsten, copper, gold, zinc, lead, nickel, silver, jade and gemstones. A scarcity of recent geological mapping available in published form, coupled with an unfavourable political climate, has resulted in the fact that although characterized by several world-class deposits, the nation's mineral resource sector is underdeveloped. As well as representing a potential new search space for a range of commodities, many of Myanmar's known existing mineral deposits remain highly prospective. Myanmar lies at a crucial geologic juncture, immediately south of the Eastern Himalayan Syntaxis, however it remains geologically enigmatic. Its Mesozoic-Recent geological history is dominated by several orogenic events representing the closing of the Tethys Ocean. We present new zircon U-Pb age data related to several styles of mineralization within Myanmar. We outline a tectonic model for Myanmar from the Late Cretaceous onwards, and document nine major mineralization styles representing a range of commodities found within the country. We propose a metallogenetic model that places the genesis of many of these metallotects within the framework of the subduction and suturing of Neo-Tethys and the subsequent Himalayan Orogeny. Temporal overlap of favourable conditions for the formation of particular deposit types during orogenic progression permits the genesis of differing metallotects during the same orogenic event. We suggest the evolution of these favourable conditions and resulting genesis of much of Myanmar's mineral deposits, represents a single, evolving, mineral system: the subduction and suturing of Neo-Tethys.

1. Introduction

Myanmar (Burma) is a highly prospective but poorly explored orogenic terrane. Despite limited past exploration, it is known to be well endowed in a diversity of mineral deposits, hosting important known reserves of varying economic significance of tin, tungsten, copper, gold, zinc, lead, nickel, silver, jade and gemstones (e.g., Barber et al., 2016; Chhibber, 1934; Coggin Brown, 1936; Gardiner et al., 2014; Griffith, 1956; Soe Win and Malar Myo Myint, 1998). The country contains ore deposits of global significance, notably Mawchi (tin-tungsten), Monywa (copper) and Bawdwin (lead-zinc); it produces some of the World's finest rubies sourced from Mogok; and is the principal global source of true jade (jadeite). A majority of Myanmar's known mineral endowment was discovered and developed during the early part of the 20th Century, however there has been comparatively little recent exploration and discovery. There is a lack of available published geological literature on Myanmar, and the country is underdeveloped with regards to the exploitation of its natural resources (e.g., Cox et al., 1981). However, as well as being a potential new search space for a range of commodities, many of its known mineral deposits remain highly prospective due to a past political and economic climate that has rendered much of its extractive industry as essentially artisanal.

Myanmar lies at a crucial geologic juncture where the main Tethys-related suture zones swing south around the Eastern Himalayan Syntaxis into Southeast Asia, with the consequence that the region has experienced an increasingly oblique collisional geometry over its Mesozoic-Cenozoic orogenic history. An understanding of both the genesis of

Myanmar's mineralization, and of its mineral potential, can only be fully realized with an understanding of its tectonic history. Myanmar, however, remains geologically enigmatic, in part due to its relative political and scientific isolation over the past half century. A number of foreign-led projects have contributed over the years to the understanding of the geological history of Myanmar: key regional re-mapping by the United Nations Directorate of Geological Survey and Mineral Exploration team (UNDP, 1978); missions by several governmental agencies (principally the Bundesanstalt für Geowissenschaften und Rohstoffe (BGR); the Institute of Geological Sciences (IGS, now BGS); and in the 1980s the Australian Development Assistance Bureau); and ongoing work by notable individuals. However, little modern dating work, using current palaeontological or radiometric techniques, or significant and accessible geological (re)mapping, has emerged from the country. Therefore, there remains considerable uncertainty around the configuration, nature and timing of major Tethyan-related tectonic events, which renders discussions on Myanmar's metallogenesis somewhat equivocal.

We propose that Myanmar has experienced a Late Mesozoic-Cenozoic orogenic event that operated over a reasonably short period of time with little overprinting complexity, yet an orogenic system that was potentially responsible for the genesis of a significant range of mineral deposits. The preservation potential of Myanmar's near-surface, epizonal mineral deposits is relatively high due to its recent geological evolution. Myanmar therefore may represent an exceptional scientific test case, affording workers the opportunity to use the tectonothermal evolution of the country to explore fundamental

questions on the relationship between a complex and evolving orogen and the resulting metallogenesis.

In this paper we review the range of known mineral deposits found within Myanmar, and place them within a space-time construct that reflects Myanmar's Mesozoic-Cenozoic geological history. We review and agree with a simple tectonic scenario: the subduction and suturing of the Neo-Tethys and the ensuing Himalayan Orogeny. We present a metallogenic model for Myanmar that accommodates the potential genesis of up to nine major metallotects within this orogenic framework. Finally, we use this model to make large-scale observations regarding the progression of orogeny and concomitant mineral deposit genesis. This thesis, if correct, would place the genesis of a majority of Myanmar's mineral deposits within a single, evolving, mineral system: the subduction and suturing of the Neo-Tethys.

1.1. A Short History of Mining and Exploration in Myanmar

Although artisanal mining and smelting of tin, silver and other deposits, by both Burmese and Chinese, occurred within what is now modern-day Myanmar during medieval times, much of Myanmar's known minerals resources were developed and exploited during the second half of the 19th century into the 20th century. Under British colonial control, the early 20th century showed a major upturn and industrialization of the Burmese mining industry, with many major mines of a variety of commodities being developed during this time, largely producing for export. Myanmar was an important producer of tungsten, a strategic war material, during the interwar period (principally supplied by the Mawchi Mine), and of lead, zinc and silver from the Bawdwin Mine in the Shan States. It was also a major supplier of tin. Much of

colonial Burma was under military occupation by the Japanese during the Second World War, who operated some of the major mines during the period 1942-44. The post-war period saw the newly independent Burma continue to produce and export a range of commodities, although production never reached pre-war levels. In 1962, General Ne Win led a military coup entrenching the rule of the Burmese army, leading to the launch of the "Burmese Way to Socialism". This process pursued the full nationalization of the Burmese economy, and a policy of economic isolation from the rest of the World. The economic effects on the mining industry were profound: all mines in Burma were brought under government control, and many commodities only became available on the black market. This period hastened the decline of the Burmese mining industry and marked a shift into largely artisanal operations, still seen today.

In 1988 Myanmar passed foreign investment legislation allowing external financial and technological investment into country. Since then, and in contrast to the minerals industry, the oil and gas sector has seen significant overseas investment. In 1994 a new Mining Law was put into place, repealing colonial-era and post-independence legislation. The new law allowed prospecting, exploration and production permits. A revision of this mining law was signed in January 2016.

1.2. Mineral Systems

Mineral deposits are heterogeneously dispersed over both space and time, reflecting both the influence of geodynamic setting on mineralization, and the transient nature of the specific geological processes that form ores (Begg et al., 2010; Cawood and Hawkesworth, 2013; Goldfarb

et al., 2005). For many mineral systems the style and timing of tectonic events are fundamental for developing the crustal architecture that accommodates mineralization. Therefore, by integrating the geodynamic evolution of a region with mineral systems theory (Fraser et al., 2007), we can place deposit models and deposit types within the context of earth evolution and provide a broad scale predictive framework for a terrane. A practical approach is to unpick an orogen on a time-integrated basis and chart the evolution of deposit types, and by inference, key mineral system elements, through the lifetime of the orogen. Due to the intricate relationships between mineral deposits and setting, such studies can ultimately better constrain the model of the orogenic system. In this paper we take this approach with Myanmar.

2. Geological Framework of Myanmar

2.1. Regional Tectonic Framework

The Mesozoic-Recent geology of Southeast Asia is dominated by the accretion of several continental micro-plates and island arc terranes that rifted from Gondwana, migrated and eventually sutured onto the South China Craton (reviews in Hall, 2012, and Metcalfe, 2013). This history of rifting and suturing represents the staged closing of the Tethys Ocean, rendering much of Southeast Asia a collage of continental blocks separated by suture zones (Fig. 1). Sibumasu (Metcalfe, 1984) is the continental microplate interpreted to underlie much of eastern and central Myanmar. Sibumasu possibly originated from the proto-Tethys margin of Gondwana, a margin postulated as having been sited above an Andean-type subduction setting during the early Palaeozoic (e.g., Cawood et al., 2007; Metcalfe,

2011b; Zhu et al., 2012). Cambro-Ordovician magmatism associated with this subduction setting (e.g., Wang et al., 2013) has been proposed as being responsible for the development of the Bawdwin Mine, a major Pb-Zn VMS-type deposit now located within Sibumasu (review in Gardiner et al., 2016). Sibumasu is interpreted to have rifted off from Gondwana in the Late Carboniferous-Early Permian (Metcalfe, 2006), subsequently colliding with the Indochina Terrane during the Indosinian Orogeny. Fig. 2 (taken from Metcalfe, 2011) is a palaeogeographic reconstruction of eastern Tethys during Jurassic-Eocene times, highlighting the Sibumasu block accreted onto Indochina and South China, and charting the development of the Neo-Tethys Ocean, and the onset of the India-Asia collision.

Myanmar has been affected by at least two major Tethyan plate collisions related to the closure of the Palaeo-Tethys and the Neo-Tethys oceans, represented by the Triassic-Early Jurassic Indosinian and Cenozoic Himalayan orogenies respectively. The result is that several major Tethyan-related metamorphic belts extend from the Eastern Syntaxis southwards across Myanmar, and which may be correlated with those lying further west along the main India-Asia collision zone (Searle et al., 2016).

The Late Triassic closure of Palaeo-Tethys and the collision of Sibumasu with the mainland (Asia) Indochina terrane resulted in the Indosinian Orogeny. The Palaeo-Tethyan suture zone is interpreted to lie in a north-south band cutting through Yunnan, eastern Myanmar, central-western Thailand and the central Malay Peninsula (Barr and Macdonald, 1991; Gardiner et al., 2015a; Metcalfe, 2002, 2000; Mitchell, 1977; Ng et al., 2015; Sone and Metcalfe, 2008; Zi et al., 2012). This suture zone forms the

boundary between two major north-south Mesozoic-age granite provinces that run across much of Southeast Asia: the *Eastern Granite Belt* and the *Central Granite Belt* of Cobbing et al. (1986). Mineralization processes associated with Central Granite Belt magmatism are responsible for most of the extensive tin deposits exploited in Malaysia and Thailand as both primary and placer deposits (Cobbing et al., 1992; Hutchison and Taylor, 1978).

The early Eocene closure of the Neo-Tethys resulted in the collision of the Indian Plate with Asia along the main convergent margin, and the subsequent onset of the Himalayan Orogeny. Suturing between India and Asia has been dated along the Indus Tsangpo (India-Asia) suture along the main Himalayan-Karakoram collision zone at 50 Ma (Garzanti et al., 1987; Green et al., 2008; Searle and Morley, 2011; Searle et al., 1988). Further east, this suture zone wraps around the Eastern Himalayan Syntaxis at Namche Barwa, and some interpret it to reappear along the Mount Victoria-Kawlun Belt in western Myanmar (see review in Searle et al., 2016). The Himalayan Orogeny resulted in significant regional crustal thickening, and the formation of major mountain belts, manifest in Myanmar as regional metamorphism (Mitchell, 1993; Morley, 2012; Searle and Morley, 2011; Sone and Metcalfe, 2008).

The collisional geometry along the main northern Himalayan suture zone, driven by the continued northwards progression of the Indian plate, is orthogonally convergent. For Southeast Asia, however, the ongoing collision occurred within the framework of a clockwise rotation of accreted Asiatic terranes around the Eastern Himalayan Syntaxis, which led to an increasingly oblique collision zone with time (e.g., Replumaz and Tapponnier,

2003). However, the amount of Cenozoic rotation varies considerably between different plate reconstructions, with the reconstructions of Hall (2012) and Zahirovic et al. (2014) suggesting much less clockwise rotation than the reconstruction of Replumaz and Tapponnier (2003). As a consequence, oblique collision for Myanmar specifically and Southeast Asia in general is an early feature of the deformation in the models of both Hall (2012), and Zahirovic et al. (2014). The oblique nature of the collision is reflected in a number of significant regional strike-slip faults that developed during the Palaeogene and Neogene, and which provided an accommodation of strain associated with this rotational history. The active tectonics of Myanmar is dominated by major strike-slip faulting along the right-lateral Sagaing Fault, and other strike-slip faults to the west (Maurin and Rangin, 2009), and strike-slip, thrust and normal fault earthquakes, associated with a relic subducted slab, dipping eastwards under Central Myanmar. Movement on the Sagaing Fault (Fig. 1), has been measured using GPS processing at a present-day ca. 1.8–2 cm/yr of strike-slip component (Maurin et al., 2010; Socquet et al., 2006; Vigny, 2003), a figure that accommodates approximately 50% of the current northwards progression of the Indian Plate. The Sagaing Fault extends south into the Andaman Sea, where it links to the Pliocene-Recent back-arc spreading centre.

2.2. Geological Provinces of Myanmar

Here we divide Myanmar into four major geological provinces from west to east (Fig. 3): the *Indo-Burman Ranges*, the *Wuntho-Popa Arc*, the *Mogok-Mandalay-Mergui Belt*, and the *Shan Plateau*.

The Indo-Burman Ranges in the far west comprise ophiolitic and Upper Triassic flysch outcropping both within the Mount Victoria Belt and elsewhere (Brunnschweiler, 1966; Mitchell, 1993). West of the Indo-Burman Ranges lies the effective margin of Asian continent (Ghose et al., 2014; Mitchell, 1993; Mitchell et al., 2012). The nature of the continental crust underlying western Myanmar is, however, disputed (see Section 5.2.2).

A 500 km-long arcuate N-S belt of Mesozoic to Neogene intrusive and volcanic rocks and Pliocene-Quaternary calc-alkaline stratovolcanoes (Mounts Popa, Taung Thonlon and Loimye) defines the Wuntho-Popa Arc (henceforth “WPA”). The WPA is a continental magmatic arc (Fig. 3) (Mitchell and McKerrow, 1975; UNDP, 1978), and comprises major Cretaceous-Eocene granodiorite intrusions with associated volcanic rocks, and middle Miocene rhyolites and dacites, principally outcropping in Mount Popa and outliers to the south (Barley et al., 2003; Khin Zaw, 1990; Mitchell and McKerrow, 1975; Mitchell et al., 2012). In places these assemblages are overlain by Quaternary basaltic andesites and pyroclastic flows (Maury et al., 2004; Stephenson and Marshall, 1984). The WPA is exposed in two principal segments, both surrounded by Oligocene-Recent shallow marine sedimentary rocks that cover much of the Arc: the 160 km-long Wuntho-Banmauk segment in the north (UNDP, 1978), and the Monywa-Salingyi segment in central Myanmar. These magmatic units intrude pre mid-Cretaceous pillow basalts, greenstones, and amphibolite and gneissic basement of undetermined age (Mitchell et al., 2011, 2012).

The WPA lies above the active easterly-dipping Burma Seismic Zone, where earthquakes have been recorded to depths of 230 km (Stork et

al., 2008; review in Searle and Morley, 2011). However it is uncertain whether the Burma Seismic Zone is underlain by a subducting slab of oceanic lithosphere, seismic receiver functions reveal that the Moho lies at 35-38 km depth beneath the southern Shillong Plateau (Mitra et al., 2005). Thus it seems probable that the Indo-Burman Ranges are underlain by continental crust that thins towards the east, with transitional oceanic lithosphere attached to the subducted plate along the Burma Seismic Zone.

The Mogok Metamorphic Belt (Searle and Ba Than Haq, 1964) is a north-south aligned belt of metamorphic rocks and granites that extends from the Andaman Sea through Mandalay northwards in an arcuate trend towards the Eastern Himalayan syntaxis (Fig. 3). It comprises a sequence of high-grade meta-sedimentary and meta-intrusive rocks, representing a regionally metamorphosed amphibolite-grade belt (Iyer, 1953; Mitchell et al., 2007; Searle et al., 2016, 2007). Zircon and monazite U-Pb dating has indicated that sillimanite-grade metamorphism is of Eocene age and younger (Searle et al., 2007). The adjacent Slate Belt (Mitchell et al., 2004) outcrops from Mandalay south towards Phuket, and is a predominantly late Palaeozoic succession of low-grade metasedimentary units; pebbly mudstones and wackes with occasional limestones, collectively defined as the Mergui Group (Mitchell, 1992). The Mogok Metamorphic Belt and Slate Belt together lie to the west of the Paung Laung-Mawchi Zone (Fig. 1). The Paung Laung-Mawchi Zone is interpreted by Mitchell et al. (2012) as a possible pre-Permian suture, consisting of folded late Jurassic to mid-Cretaceous marine clastic sedimentary rocks and limestones. Intruding into both of these units is Myanmar's second major magmatic belt, a north-south trending belt of

granitoids emplaced from the Late Cretaceous to at least Eocene times (Barley et al., 2003; Cobbing et al., 1992; Mitchell et al., 2012; Searle et al., 2007). This has been variously termed the Western Province (Cobbing et al., 1992) - which is a confusing term within the context of Myanmar as it lies to the central-east of the country - or the Central Granitoid Belt (e.g., Khin Zaw, 1990). Here we refer to the entire zone comprising Mogok Metamorphic Belt rocks, plus the Slate Belt (Mergui Group) and all granites east of the Sagaing fault and west of the Paung Laung-Mawchi Zone, as the *Mogok-Mandalay-Mergui Belt* (MMM Belt).

The fourth province, the *Shan Plateau* in eastern Myanmar, consists of Cambrian-Ordovician sedimentary sequences with localized Ordovician volcanic rocks and volcaniclastics (Aye Ko Aung, 2012), unconformably overlain by thick Middle-Upper Permian limestone sequences. These latter sequences may represent the protolith carbonates of the high-grade Mogok marbles. The boundary between the MMM Belt and the Shan Plateau sequences is marked by the Shan Scarps and the Paung Laung-Mawchi Fault Zone (Garson et al., 1976). However, some workers have postulated the existence of a cryptic suture along this boundary. The boundary has been suggested to have developed either as (a) a consequence of the closure of the Neo-Tethys thrusting the Precambrian to Cambrian Chaung Magyi Formation of the Shan Plateau sequences over the Slate Belt (the so-called “Medial Suture Zone” of Mitchell et al. (2015)) or (b) a major strike-slip fault (Ridd, 2016), marking the boundary of the “Phuket-Slate Belt Terrane” of Ridd and Watkinson (2013). Although the existence of such a suture would have major implications for the western extent of the Sibumasu

basement (Section 5.2.1), it is nevertheless likely that continued crustal shortening and basin closure up to Late Cretaceous times (Mitchell et al., 2015), were responsible for juxtaposing the Shan Plateau and the MMM belt, resulting in the formation of contiguous basement during the Cenozoic.

3. U-Pb Geochronology

We collected several samples of magmatic rocks for zircon U-Pb geochronology that are relevant to some of the mineralization types discussed here (Table 1). Granite samples MY34 and MY37 were taken from quarries close to the Dawei tin district, sample MY76 from a quarry immediately north of Myeik, all within the southern MMM Belt. Sample MY-YAD is from the Yadanabon Mine, a primary and elluvial Sn mine in southern Myanmar, close to the Thai border (also within the MMM Belt).

MY106 is a sample of the Kabaing Granite, a peraluminous biotite granite intruding the Mogok Metamorphic Belt, and which is associated with localized base metal skarn-type mineralization (Tin Aung Myint et al., 2014). Sample MY145 is the diorite that hosts Cu-Au porphyry-type mineralization at Shangalon, lying within the southern part of the Wuntho Batholith in the WPA.

3.1. Method

Zircons grains from all samples were separated using a combination of heavy liquid and Frantz magnetic separation techniques. Selected zircons were then mounted in epoxy and imaged using a FEI Quanta 650 FEG Scanning Electron Microscope at the Department of Earth Sciences, University of Oxford.

All samples except MY106 were analyzed using the large geometry CAMECA IMS1280 ion microprobe at the NordSIM Facility housed at the Swedish Museum of Natural History, Stockholm, Sweden, using methods similar to those described by Whitehouse and Kamber (2005) and Whitehouse et al. (1999). MY106 was analyzed at the NERC Isotope Geosciences Laboratory, Keyworth, UK (NIGL), using a Nu Instruments Attom single-collector ICP-MS coupled to a New Wave Research 193UC excimer laser ablation system. The full method is described in Spencer et al. (2014).

All results used Isoplot for data presentation (Ludwig, 2004). All calculated ages are $^{206}Pb/^{238}U$ ages presented at 2σ, and include propagation of analytical and systematic uncertainties. Concordia and weighted average diagrams are presented in Fig. 4. Full zircon results are detailed in Table 2.

3.2. Results

The age for most samples is determined from the intersection of a regression line through uncorrected data, which is anchored at the modern day initial-Pb value ($^{207}Pb/^{206}Pb$ = 0.83; Stacey & Kramers (1975)), and the concordia curve (Fig. 4). The composition of common Pb has been demonstrated as appropriate for the NordSIM laboratory (Kirkland et al., 2008). As the majority of data (when ^{204}Pb corrected) is near concordant, this form of common Pb correction does not result in significant differences to the calculated ages.

3.2.1. Sample MY34

MY34 is composed predominantly of quartz, alkali feldspar, and minor plagioclase and biotite. 20 analyses were performed on 18 grains. Analyses uncorrected for common Pb are concordant to significantly normally

discordant, principally reflecting a mixture between radiogenic and common Pb (Fig. 4A). Two data points lie to the left of regression line and yield slightly older ^{207}Pb corrected ^{238}U/^{206}Pb ages of 65.3 and 65.4 Ma (blue, Fig. 4A). These analyses are interpreted to represent xenocrystic zircon and hence date a somewhat older inherited component within the granite (Spot IDs 02 & 17). The remaining 19 analyses define one coherent group, based on their ^{238}U/^{206}Pb and Th/U ratios (0.1-1.0), for which the regression line intersects the concordia curve at 62.3 ± 0.6 Ma (MSWD 2.1), interpreted as the magmatic crystallization age of the granite (Fig. 4A).

3.2.2. Sample MY37

Sample MY37 is quartz + alkali feldspar dominated, with plagioclase and occasional biotite. It also contains obvious pyrite. 19 analyses were performed on 11 grains. Zircon crystals from MY37 indicate variable U concentrations. Four data points with a U concentration <500ppm have a UO_2/U ratio within the range of the standard run during the session, hence their U/Pb ratio is regarded as robust. These four analyses when fitted with a regression from a modern day common Pb value yield an intersection with the concordia curve at 69.5 ± 1.0 Ma (MSWD 1.9), interpreted to reflect magmatic crystallization of the granite (Fig. 4B). The remaining 14 data points with higher U contents have a UO_2/U ratio outside the range of the standard for the session, reflecting the difference in sputtering characteristics of the 91500 zircon standard relative to high U zircon (e.g. matrix matching effect; Kirkland *et al.* 2008). Nonetheless, the high U content results in high counts of radiogenic Pb and we use the ^{207}Pb/^{206}Pb age in preference because it is not dependent on the U/Pb calibration. The weighted average ^{204}Pb corrected

$^{207}Pb/^{206}Pb$ date from the high U analyses is 70 ± 13 Ma (MSWD = 2.5), which is in close accord with the age calculated from the regression through common Pb and low U zircon (Fig. 4B).

3.2.3. Sample MY76

Sample MY76 is also a biotite granite, comprised of a matrix dominated by quartz, alkali feldspar and plagioclase, plus minor biotite. 14 analyses were performed on 10 grains. All points from sample MY76 have extreme U contents, in some cases > 35,000 ppm. These analyses are outside the UO_2/U range of the standard during the session. Hence, in order to calculate a meaningful age from this sample we use the weighted mean ^{204}Pb corrected $^{207}Pb/^{206}Pb$ age, which yields a date of 75.3 ± 7.7 Ma (MSWD 1.8), interpreted as the age of magmatic crystallization (Fig. 4C).

3.2.4. Sample MY-YAD

MY-YAD shows a typical composition to the other MMM belt granites: quartz, alkali feldspar plus plagioclase, with occasional biotite now heavily altered to chlorite. 18 analyses were performed on 14 grains. The analyses are concordant to discordant, principally reflecting a mixture between common and radiogenic Pb. One data point lies significantly to the right of the regression line and yields a younger ^{207}Pb-corrected age, interpreted to reflect the effects of recent radiogenic-Pb loss (spot ID n5105-02; Fig. 4D). 12 data points with high (or extreme) U content >2000ppm (blue, Fig. 4D), and a UO_2/U value outside the range of the standard used for U/Pb calibration during the analytical session, are also excluded from the regression. The remaining 5 data points yield a regression from common Pb

which intersects the concordia curve at 50.3 ± 0.6 Ma (MSWD 1.3), interpreted as the magmatic crystallization age of the granite (Fig. 4D).

3.2.5. Sample MY106

Sample MY106 is a medium-grained biotite granite. 17 analyses were performed. The analyses define two populations an older concordant population and a younger component that reflects a mixture between radiogenic and common Pb. Two data points lie significantly to the left of a regression line and yield older ^{207}Pb-corrected ages of 46.2 ± 0.6 Ma and 45.3 ± 0.6 Ma (blue in Fig. 4E). These analyses are interpreted to reflect inheritance. 2 analyses lying slightly to the right of the regression line yield ^{207}Pb corrected ^{238}U/^{206}Pb ages of 15.6 ± 0.4 Ma and 15.8 ± 0.3 Ma (Spot IDs 4 & 6) and are interpreted to have undergone a minor amount of geologically recent radiogenic-Pb loss (red in Fig. 4E). The remaining 13 data points fit a regression line which intersects the concordia curve at 16.8 ± 0.5 Ma (MSWD 1.9), including propagation of analytical uncertainty. This is interpreted as the magmatic crystallization age of the granite.

3.2.6. Sample MY145

Sample MY145 is a medium-grained quartz diorite with plagioclase plus quartz, and relic hornblende. 14 analyses were performed on 10 grains. One analysis lies to the left of a regression from common Pb and yields an older ^{207}Pb age of 42.5 ± 0.7 Ma (spot ID n5329_08; Fig. 4F). This analysis was located on a separate grain and is interpreted to reflect inheritance. The remaining 13 data points fit a regression from common Pb that intersects the Concordia curve at 40.2 ± 0.2 Ma (MSWD 1.03), interpreted as the magmatic crystallization age of the granite.

4. The Mineral Endowment of Myanmar

Workers have classified Myanmar's mineral deposits into a variable number of distinct metallotects, distinguished largely on the basis of either tectono-stratigraphic association, or by commodity endowment (Bender, 1983; Chhibber, 1934; Gardiner et al., 2014; Goossens, 1979; Mitchell and Htay, 2013; Ko Ko Myint, 1994; Soe Win and Malar Myo Myint, 1998). Here we outline nine distinct metallogenic provinces for discussion (Table 3). While collectively these do not represent an exhaustive list of Myanmar's total mineral endowment, they reflect the relevant and known set of deposit types within Myanmar that can potentially be linked to the Tethyan metallogeneic model discussed here.

4.1. Magmatic-Hydrothermal Granite and Pegmatite-Hosted Sn-W

Southern Myanmar contains extensive, world-class tin and tungsten mineralization, principally focused in a north-south trending belt that extends from east of Yangon southwards along the Myeik Archipelago (Fig. 3). Primary deposits are strongly associated with the intrusion of Late Cretaceous-Eocene granites of the MMM Belt intruding metasedimentary rocks of the Slate Belt (Chhibber, 1934; Hutchison and Taylor, 1978; Khin Zaw, 1990). Primary tin mineralization in Myanmar is found as cassiterite-hosting quartz veins and as significant pegmatites, either within the country rock, or the upper parts of the granite intrusions. The principal tin-producing area is located around the port town of Dawei (Tavoy), where ca. 50 primary deposits are located (Fig. 3). Much historical production was alluvial/elluvial, and these deposit types are particularly focused around Myeik (Mergui) in the

far south (Coggin Brown and Heron, 1923; Coggin Brown, 1918; UNDP, 1996).

This metallogenic province is also rich in tungsten, found spatially associated with the tin mineralization commonly as wolframite, and more rarely as scheelite. In some deposits tungsten contents are found to exceed tin, and there appears to be a geographic zonation in Sn:W ratio (e.g., Hobson, 1940). The Mawchi Mine, located 250 km northeast of Yangon, was once a globally significant tungsten mine, briefly delivering 10% of global tungsten production during the interwar period (Khin Zaw and Khin Myo Thet, 1983).

Although tin-bearing granite compositions are broadly peraluminous (S-type) (Khin Zaw, 1990), there is a geographic variation in the degree of differentiation (Cobbing et al., 1992; Khin Zaw, 1990; Pollard et al., 1995; Sanematsu et al., 2014). Sanematsu et al. (2014) reported that relatively older Late Cretaceous to Palaeocene granites to the east of the N–S striking Dawei fault are more siliceous and more highly fractionated (i.e. typically S-type), whilst younger Palaeocene to Eocene granites to the west are less fractionated and more oxidized, implying a trend towards a I-type affinities with time.

4.2. Skarn-Type Au-Ag

Native gold and base metal sulphide mineralization is found hosted within the phlogopite-bearing amphibolite-grade marbles of the Mogok Metamorphic Belt. Approximately 50 km south of Mogok lies the Shante Gold District, a 500 km^2 marble-hosted gold province spatially associated with the emplacement of peraluminous granites. Mineralized quartz veins intrude the

marbles, and host base metal (Zn+Pb) sulphides and native Au up to 5 ppm (Tin Aung Myint et al., 2014).

The Kwinthonze Mine, near Thabeikkyin, is a marble-hosted Au-base metal sulphide deposit with accessory garnet and wollastonite, interpreted as a skarn-type deposit, and through spatial association, thought to be linked to the intrusion of the Kabaing Granite (Tin Aung Myint et al., 2014). The Kabaing Granite (sample MY106) we have dated through zircon U-Pb geochronology to ca. 17 Ma, which we interpret as providing some age constraint on this mineralization, and related to the late stages of Mogok metamorphism.

4.3. Porphyry-Type Cu-Au

Within the WPA base metal (Cu) sulphide and Au deposits have been documented since at least since the 1930s (e.g., Chhibber, 1934). Two principal types of deposits have been found within the WPA: porphyry Cu-Au and high-sulphidation epithermal-polymetallic (Au-Cu) styles (UNDP, 1996).

Near Wuntho, porphyry-style Cu-Au deposits occur, notably at Shangalon in the south of the massif (Fig. 3). Mineralization is intimately associated with magmatic intrusions (Hammarstrom et al., 2010; Mitchell et al., 1999; UNDP, 1996). The main Wuntho granodiorite batholith has been dated through U-Pb zircon geochronology to the Cretaceous (ca. 95 Ma) (Barley et al., 2003; Mitchell et al., 2012). However, mineralization at Shangalon is spatially associated with the Eocene intrusion of finer-grained micro diorite into the hosting batholith. The hosting diorite is here dated using U-Pb in zircon geochronology at 39.9±0.31 Ma (sample MY145), providing an approximate estimate for the age of mineralization. Porphyry-type

mineralization has been reported elsewhere in the Wuntho area (Goossens, 1979; UNDP, 1978), but have no definitive age constraints.

4.4. Epithermal Au-Cu

Epithermal Au-Cu mineralization has been recognized at several localities within the WPA (Goossens, 1979; UNDP, 1996). Auriferous quartz veins have been reported near Wuntho. They are hosted both by the granodiorite and diorite magmatic rocks, and by the country rocks, and mineralization has been interpreted as being at latest of Cretaceous age (Mitchell et al., 1999). However, geochronology suggests that some epithermal-type deposits in the WPA may be of Miocene-age. The Monywa Cu Mine further south, which includes the giant Leptadaung deposit, has been interpreted as a high-sulphidation epithermal deposit, and is characterized by the absence of economic-grade Au (Mitchell et al., 2011). The same workers inferred an age of formation for Monywa of mid-Miocene on the basis of U-Pb radiometric age dating of a local dyke.

Historically, most Au production in the northern WPA region has been from high-grade auriferous quartz veins, found both in the granodiorites and surrounding host rocks, and from derived placers in the northerly Wuntho and Tagaung-Myitkyina segments of the WPA (Chhibber 1934; Mitchell et al, 1999).

4.5. Ultramafic-hosted

Ultramafic-hosted deposits within Myanmar are focused around the various ophiolite fragments found within the country. The poorly-studied Tagaung-Myitkyina Belt (TMB) lies between the Mogok Metamorphic Belt and the Katha-Gangaw Belt (KGB) in the north of the country (Fig. 3). Outcropping

along the eastern bank of the Irrawaddy River in the Kyawbingyon Region, the TMB comprises significant ophiolitic mantle peridotite (Searle et al., 2016). Extreme weathering of these TMB ultramafic rocks has resulted in lateritic concentrations of non-sulphide nickel. The large Tagaung Taung Mine, 200 km north of Mandalay, is a major nickel laterite deposit that was discovered by BGR geologists in the early 1980s. At Tagaung Taung the laterites are associated with outcrops of precursor dunite, harzburgite and serpentinite (Schellmann, 1989).

The Jade Mines Belt (JMB, Fig. 3), another metamorphic belt, lies along the northern segments of the Sagaing Fault. The Jade Belt is a high-P subduction-related assemblage (Goffe et al., 2002). Although dominated by outcrops of peridotite and serpentinite, it remains poorly exposed and little studied. The majority of mined jade is sourced from bounders in young alluvial deposits along the Uru River (e.g., Hughes et al., 2000). A variety of jade rock assemblages have been reported: pure jadeitite, amphibole jadeite, omphacite-jadeite-zoisite-kyanite and kosmochlor (Franz et al., 2014; Goffe et al., 2002). The Hpakant region is globally unique in the extensive occurrence of pure jade, jadeite (Hughes et al., 2000).

Chromite and nickel deposits have been recognized in the ultramafic rocks of the Western Ophiolite Belt (Section 5.3) within the Chin and Naga Hills (Bender, 1983; Chhibber, 1934).

4.6. Orogenic-Type Au

Gold mineralization has been recognised at numerous localities throughout the Slate Belt (e.g., Bender, 1983; Mitchell et al., 1999; Zaw Naing Oo and Khin Zaw, 2009). Although neither its genesis nor age is well

constrained, workers have inferred the mineralization to be of Orogenic type (Khin Zaw et al., 2014; Mitchell et al., 2004). Several deposits have been studied. The Meyon gold deposit in southern Myanmar is interpreted as structurally controlled, and related to movement on the Papun Fault Zone (Zaw Naing Oo and Khin Zaw, 2009). The same workers bracketed the age of mineralization as Late Cretaceous to Palaeogene.

However, the most detailed study to date of this mineralization style in Myanmar has been undertaken at the Modi Taung-Nankwe Gold District in central Myanmar, where Au mineralization is associated with quartz-pyrite stringers and veinlets cutting the Slate Belt. Mitchell et al. (2004) suggested that at Modi Taung, gold mineralization was related to the ascent of metamorphic fluids following prograde metamorphism of the Mogok Metamorphic Belt, which they inferred to be of Jurassic Age, but which has since been dated by monazite U-Pb geochronology as Eocene-Oligocene in age (Searle et al., 2007). However, older age constraints on Slate Belt gold mineralization have been proposed, as discussed in Section 6.2.3.

4.7. Sediment-hosted Pb+Zn Sulphide Deposits

Several significant carbonate-hosted Pb-Zn sulphide deposits have been reported from the Upper Palaeozoic carbonate sequences of the Shan Plateau. The Theingon (or Bawsaing) Pb+Zn+Ag Mine in the Southern Shan States has been interpreted as a stratabound carbonate-hosted Mississippi Valley Type (MVT) or Irish type deposit of Ordovician age (Khin Zaw et al., 2014, 1984).

4.8. Gemstones

Arguably the World's finest rubies are sourced from the stone tracts of Mogok in central Myanmar, hosted by the metamorphic rocks of the Mogok Metamorphic Belt. Gem-quality rubies and sapphires are derived from corundum ± phlogopite ± clinopyroxene ± forsterite ± spinel-bearing marbles both around Mogok, and north of Mandalay (Bender, 1983; Chhibber, 1934; Iyer, 1953; Mitchell et al., 2007; Searle and Ba Than Haq, 1964; Searle et al., 2016, 2007; Themelis, 2008). These gemstones have withstood the processes of extreme lateritization, and are now largely found in outcrop and enclosed in tropical red soils known locally as *byons* from which they are mined.

Gem rubies are thought to form through the thermal reduction of evaporites during high temperature, medium pressure metamorphism of platform carbonates (Garnier et al., 2008). The evaporite sequences contain sufficient trace element contents of Al and Cr derived from entrained clay material to produce ruby, a form of corundum. Topaz, tourmaline and aquamarine (beryl) are mined from pegmatite dykes that are associated with the Kabaing Granite that intrudes the marbles immediately west of Mogok town (e.g., Iyer, 1953).

Age determinations of both pelites, and from metasomatic rubies found in the marbles, has led to the interpretation of two peak amphibolite-grade Mogok metamorphic events – one occurring in the Palaeocene and the other during the Eocene-Oligocene (Searle et al., 2007). $^{40\text{-}39}$Ar cooling ages from phlogopite found in the Mogok marbles have yielded Miocene ages (18.7-17.1 Ma; Garnier et al., 2006), interpreted as the date of ruby formation.

This would imply that ruby formation occurred during an Early Miocene retrograde phase following peak amphibolite-grade Eocene-Oligocene metamorphism, although other workers believe their formation to be related to a peak metamorphic event (Searle et al., 2016). This is also similar to our magmatic age for the Kabaing granite, the intrusion of which led to pegmatite-hosted topaz and aquamarine.

4.9. Sediment-hosted Epithermal Au

The largest gold-producing mine in Myanmar is the Kyaukpahto Mine, sited in Kawlin Township, Sagaing Division. Au mineralization is associated with stockwork-style quartz veins hosted in silicified sandstones, and formed during extensional faulting. Veins comprising pyrite, chalcopyrite and arsenopyrite (Ye Myint Swe et al., 2004) are best developed in competent silicified sandstone locally extending into the adjacent mudstones of the Lower-Mid Eocene Male Formation (Mitchell et al., 1999). These host rocks have undergone intense hydrothermal alteration and silicification, which appears to be critical for the genesis of the veining, the latter generally confined to the silicified sandstone.

Fluid circulation and vein formation is most probably related to movement on the Sagaing Fault. NNE-trending extensional faults formed by a component of dextral strike-slip movement host the stockwork epithermal Au mineralisation structures (Ye Myint Swe et al., 2004).

5. Tectonic Model

We propose a Late Mesozoic-Cenozoic tectonic model that provides a framework for the discussion of metallogenesis. Key aspects for

discussion are (a) the age and tectonic relationships between the two magmatic belts, and (b) the nature and continuity of the underlying crust.

5.1. Age of Magmatic Belts

Geochronology suggests that at least two main magmatic episodes occurred within the WPA, which were followed by a Quaternary episode of andesite-dacite stratovolcanoes related either to subduction-related magmatism (Stephenson and Marshall, 1984) or slab detachment and asthenospheric upwelling (e.g., Maury et al., 2004). U-Pb geochronology from magmatic zircon analysis suggests (a) a short period of magmatism operating in the Mid-Late Cretaceous (Barley et al., 2003; Mitchell et al., 2012); (b) a magmatic Eocene event (Shangalon; our new data, and similar reported in Barley *et al.* 2003); and (c) activity in Miocene times (Mitchell *et al.* 2012).

These data raise the question of whether the WPA comprises three separate magmatic episodes, or a single long-lived event disguised for the present by the paucity of age data. Detrital zircon ages from Cretaceous to Miocene successions in the Chindwin Basin, the forearc of the Wuntho-Popa Arc, were reported by (Wang et al., 2014). Interpreting these to have WPA provenance, Wang et al. (2014) suggested their data implied a main magmatic stage for the Arc of between 110-80 Ma, and a lesser subordinate stage between 70-40 Ma. Our new age for Shangalon lies within the younger of these. Therefore, it is possible the Arc was near-continuous from the Mid-Cretaceous to Eocene times, and then experienced a late Miocene event during which the Monywa deposit formed.

U-Pb ages from the MMM Belt indicate earlier Jurassic and Triassic Indosinian-related magmatism (ca. 170 Ma; Barley et al., 2003); an

extended period of Cretaceous to Eocene magmatism (e.g., Aung Zaw Myint et al., 2016; Mitchell et al., 2012; Sanematsu et al., 2014; our new data); and leucogranites and other magmatism associated with Oligocene-Miocene metamorphism (e.g., Searle et al., 2007; our Kabaing Granite data). MMM Belt granites point to a general trend towards more S-type affinity with time (Cobbing et al., 1992). This change in magmatic style with time is perhaps related to slab rollback in a continental subduction or island arc setting (e.g., Mitchell, 1986; Mitchell and Myint Thein Htay, 2013; Sanematsu et al., 2014).

The recognition that the WPA and MMM Belt are sub-parallel magmatic belts hosting contrasting mineralization styles (Cu-Au and Sn-W respectively) prompted the consideration of their tectonic and metallogenic implication as a pair (full review in Gardiner et al., 2015b). Mitchell (1979) noted a similarity with the metallogenic belts of the South American Cordillera (Peru/Bolivia). In this analogue, the WPA would represent the intrusion of subduction-related I-type magmatism sited immediately above the plate margin, associated with porphyry and epithermal-type Cu-Au mineralisation (Fig. 5A). Thus the WPA is analogous to the coastal copper belts of the Central Andes. Conversely, the Cenozoic intrusions of the MMM Belt results from magmatism sited more distally to the plate margin, being sourced from the melting of more reduced, dominantly pelitic protoliths, and giving rise to crustal-melt S-type granites and associated lithophile tin-tungsten mineralization (Fig. 5A). The MMM Belt would therefore find a geodynamic parallel in the Bolivian tin belts, at least with commodity type, if not mineralization style *per se*.

Although there is some evidence for contemporary magmatism in the Eocene, the various styles of mineralization between and within these belts are potentially of different ages. Further, the relationship between the higher grade Mogok Metamorphic Belt containing both older and much younger magmatism, and the early Cenozoic magmatism in the Slate Belt is unclear. Despite these issues, we believe a case may still be made that the WPA and certainly the southern Slate Belt part of the MMM may represent paired magmatic belts. If so, then a tectonic setting for their petrogenesis is perhaps an Andean-type accretionary setting on the margins of a subducting Neo-Tethys during the Late Cretaceous-Eocene prior to the collision of India (Gardiner et al., 2015b; Mitchell, 1979). We adopt this framework for the ensuing discussion.

5.2. The Crustal Evolution of Myanmar

The western extent of Sibumasu is uncertain. Some workers have proposed the existence of an intermediate ocean basin, the so-called Meso-Tethys, that may depending on interpretation have separated the MMM Belt from the Shan Plateau. The nature of the crust underlying western Myanmar, including the WPA, has been the subject of recent study. Defining a feasible tectonic model for Myanmar during the Late Mesozoic-Cenozoic requires addressing these issues.

5.2.1. A Thai-Myanmar Meso-Tethys Suture?

The existence of a Meso-Tethys ocean within the area typically defined as Sibumasu has been proposed several times previously (Cooper et al., 1989; Mitchell, 1992), and has also received recent attention in the literature (Mitchell et al., 2015, 2012; Ridd, 2015). In Yunnan, a proposed

Meso-Tethys suture (Nujiang suture) forms the boundary between the Tengchong and Baoshan Blocks (see review in Burchfiel and Chen Zhiliang (2013)). One of the key differences between the blocks relates to the Palaeozoic stratigraphic column, in particular the kilometres thick nature of Carboniferous-Early Permian glacio-marine sediments on the Tengchong Block, and much less well developed nature of equivalent sediments (10's-100's m thick) in the Baoshan Block. The question is whether these stratigraphic differences can be explained by variations within a single continental block, such as thickness changes due to rifting (e.g., Ridd, 2009), or whether an ocean basin once separated the blocks. In Yunnan and Tibet the Baoshan Block is considered to be equivalent to the South Qiangtang Block, while the Tengchong Block is equivalent to the Lhasa Block, and in these areas there is clear evidence for a major ocean based on abundant arc volcanic rocks, ophiolitic remnants, and palaeomagnetic evidence for up to 31° of latitudinal separation between the Lhasa and Qiangtang blocks (Otofuji et al., 2007). Even in the better-known parts of the Nujiang suture the timing of closure is uncertain, with some arguing for an Early Cretaceous closure at around 120 Ma (Cao et al., 2014; Chen et al., 2004; Raterman et al., 2014; Zhao et al., 2015; Zhu et al., 2015, 2012) and others preferring a Late Cretaceous closure (Fan et al., 2015; Wang et al., 2015).

Similar stratigraphic characteristics as those defining the Tengchong and Baoshan Blocks are proposed to be present along a line that runs along the Paung Laung Fault in Myanmar, the Three Pagodas and Khlong Marui faults in Thailand, and the Straits of Malacca between Malaysia and Sumatra (Mitchell et al., 2015, 2012; Ridd, 2015). Ridd (2015) refers to

the western area (western Myanmar, northern Peninsular Thailand and Sumatra) as the Irrawaddy Block, and the eastern area as Sibuma. Stratigraphically, the argument seems as compelling as in Yunnan, but structural and tectonic evidence for a suture is not strong, perhaps because of overprinting by later thrusting and strike-slip motion (Ridd, 2015). On the basis of radiometric dating, Liu et al. (2016) interpreted the Eastern Belt ophiolites to be marking an extension of the Nujiang suture (see Section 5.3). Here we accept that a significant oceanic-floored rift relating to the Meso-Tethys at least partially if not completely separated Sibumasu into two separate blocks, which nevertheless seems likely to have sutured by the Late Cretaceous, based on both the models proposed by Ridd (2015) and Mitchell et al. (2012).

5.2.2. The West Burma Plate

The tectonic units to the west of the Shan Plateau have been subject to numerous interpretations. Much discussion has focused around the existence or otherwise of a separate microplate, variously described as the Burma Plate, Burma Platelet, West Myanmar Terrane, or most commonly as the *West Burma Block* (Curray, 2005; Curray et al., 1979; Metcalfe, 2011; Rangin et al., 2013). This block has been separately invoked as (a) explaining the S-type, tin-bearing granitic plutons of the MMM Belt (Charusiri et al., 1993; Hutchison, 1994); and/or (b) explaining Palaeogene deformation in the Indo-Burma Ranges (Acharyya, 2010, 2007). Its origin has also been explained as due to (a) Early Carboniferous accretion onto South China as part of Indochina, followed by strike-slip emplacement onto the western margin of Sibumasu during the mid-Cretaceous (Barber and Crow, 2009); (b) as Late Cenozoic as a result of hyper-oblique convergence, forming the region

between the Sunda Trench and the Sagaing-Sumatra fault systems (Rangin et al., 2013); or (c) only established in the Mid-Eocene as a consequence of movement along the Sagaing Fault, thereby dividing Sibumasu (Mitchell, 1993).

Assuming the West Burma Plate was a separate block, Sevastjanova et al. (2015) undertook detrital U-Pb zircon age analyses from Triassic turbidite sandstones locally overlain by pillow basalts, within the Chin Hills in western Myanmar (Fig. 3). The detrital zircons yielded Permian-Triassic magmatic ages, interpreted as being sourced from the Palaeo-Tethys related granite belts further east. They also identified chromium spinels, which are common in Southeast Asia but rare in an Australia lacking significant ophiolitic material, the likely source of this block. They concluded that both West Burma and Sibumasu together formed part of Gondwana at least until the Devonian, and that the West Burma Plate had most likely docked onto Southeast Asia before Mesozoic times.

Isotopic analysis of detrital zircons sourced from the Cretaceous-Miocene successions of the Chindwin Basin, thought to represent the forearc of the WPA, were reported by Wang et al. (2014). Zircon Hf signatures of samples with a Cretaceous-Eocene magmatic-age yielded largely radiogenic εHf values, corresponding to two stage model ages of 1.0-1.2 Ga, and suggestive of a more juvenile source for WPA magmas. Reported εHf data from eastern Sibumasu sampled in Thailand and eastern Myanmar have yielded εHf values in the range of +3.7 to – 10.5, representing Meso- to Palaeoproterozoic model ages (Gardiner et al., 2015a; Lin et al., 2013).

We suggest that these data indicate that the West Burma Block may be an artifact of movement on the Sagaing Fault, and that the continental crust underlying western Myanmar is either Sibumasu crust, or a separate block accreted possibly by the mid-Cretaceous times at the latest. This scenario allows both magmatic belts (the WPA and the MMM Belt) to have formed as adjacent parallel belts on a common continental margin, overlying the subducting Neo-Tethys.

5.3. Ophiolite Belts

Reconstruction of the Late Mesozoic-Cenozoic history of collision in Myanmar is largely dependent on interpretation of the various ophiolite fragments. Ophiolite outcrops in Myanmar are thought to comprise at least two distinct belts (Hutchison, 1975; Mitchell, 1993). The *Western Belt* (WB in Fig. 1) follows the trend of the eastern Indo-Burman Ranges, and is best described from the Naga Ophiolite (Acharyya, 2010, 2007). This belt has been interpreted to represent the final closure of the Neo-Tethys during the late Eocene (Acharyya, 2007; Ghose et al., 2014), being the eastern suture of the Indian Plate. The *Eastern Belt* (EB in Fig. 1) lies east of the Indo-Burman Ranges as fragments in both the Jade Mines Belt and in the Tagaung-Myitkyina Belt, and may include ophiolite fragments found east of the Mount Victoria Belt (Acharyya, 2007; Mitchell, 1993; Mitchell et al., 2011). The Eastern Belt has been interpreted by some to represent the earlier closure of a back-arc ocean between either a continental block (e.g., Acharyya, 2010), or an accreted volcanic arc (i.e. the Mawgyi Nappe of Mitchell (1993), and Southeast Asia.

Neither the age of oceanic crust formation, nor the timing of obduction and/or emplacement, of any of the ophiolite fragments found within Myanmar are precisely known. Some workers have placed the Western Belt ophiolites as Jurassic in age (Suzuki et al., 2004). Working in the Naga Hills, within the Western Ophiolite Belt, Ghose et al. (2014) used stratigraphic associations to infer the timing of final emplacement of the Naga Ophiolite as Eocene, although this age may reflect a later thrusting event and not the original emplacement event.

Liu et al. (2016) presented zircon U-Pb geochronology of plagiogranites and other felsic intrusions found within both the Western Belt and Eastern Belt ophiolites. They ascribed a Cretaceous age of formation to the Western Belt, and a Jurassic age to the Eastern Belt. They concluded that the Western Belt represents the trace of a southerly extension of the Yarlung-Tsangpo (Neo-Tethys) suture found within Tibet, and that the Eastern Belt shows similar ages to the Bangong-Nujian (Meso-Tethys) suture. This contradicts the model of Mitchell (1993), who proposed that the Eastern Ophiolite Belt represents a truncated northerly extension of the Western Ophiolite Belt, and which has been offset southwards by movement on the Sagaing Fault. Given modern-day slip rates, such a displacement would require ca. 450 km of fault movement, which necessitates a longer-lived fault than is currently interpreted by some workers, specifically one stretching back to the Miocene.

However, the fragments of the Eastern Belt ophiolite are discontinuous, and further there is a paucity of geological evidence south of Mogok for a major suture zone. Regardless of the pre-Cretaceous history, we

can still accommodate the concept of a continuous basement extending under Myanmar as far west as the continental margin in the Cenozoic.

6. Tethyan Metallogenesis

In line with the tectonic evolution described above, we propose a simplified orogenic model for the Mesozoic-Cenozoic geological evolution of Myanmar: an accretionary margin on the western edge of Asia, sited above the easterly subduction of the Neo-Tethys, and operating from at least the Late Cretaceous to Eocene times. Suturing of the Neo-Tethys likely occurred in the mid-late Eocene, and the ensuing Himalayan Orogeny caused concomitant crustal thickening that continued to at least the Oligocene. Ongoing rotation around the Eastern Syntaxis forced plate convergence, likely oblique at inception, to become increasingly hyper-oblique, eventually initiating movement on the Sagaing Fault, possibly as early as the Miocene, becoming a major transform boundary seen today.

6.1. Metallogenic-Tectonic Model

Mineral deposits form under specific conditions within specific tectonic and geodynamic settings (Barley and Groves, 1992; Bierlein et al., 2009; Groves and Bierlein, 2007; Kerrich et al., 2005; Mitchell and Garson, 1981). The Tethyan collision zone, resulting in the Alpine-Himalayan Orogeny, has, in places, proved a highly fertile zone for metallogenesis (e.g. review in Richards, 2014). We define four major stages of orogenic evolution in our model of the Himalayan Orogeny in Myanmar, outlined in Fig. 6. Each of these describes a specific temporally-constrained geodynamic setting as follows:

(a) *accretionary* (100-50 Ma)

(b) *collisional* (50-30 Ma)

(c) *late collisional* (30-20 Ma)

(d) *highly-oblique collisional* (15-0 Ma).

Although we define only the final stage as being oblique, we accept that the collision was likely oblique to a significant degree for much of its history. To this tectonic framework, we assign the nine major deposit types described in Section 0 on the basis of either age constraints (inferred or measured), or from geological observations that lead to an interpreted tectonic setting for its genesis. Fig. 5 shows the schematic genesis for a number of these metallotects.

6.1.1. Accretionary Stage (100–50 Ma)

An Andean-type accretionary setting on the margins of the Neo-Tethys operated in central Myanmar from the Late Cretaceous to Eocene. This setting was responsible for the generation of extensive subduction-related I-type magmatism, which was principally focused in the WPA.

Tin-tungsten mineralization is located where granites of the MMM Belt intrude the Slate Belt (e.g. at Hermyingyi, Mawchi and Yadanabon). Zircon U-Pb studies indicate crystallization ages of both mineralized and presumed coeval non-mineralized granites within the MMM Belt are largely of Palaeogene age. Our zircon U-Pb ages of 75–50 Ma (MY34, MY37, MY76, and MY-YAD) from granites within the southern MMM belt that are either within the Dawei vicinity and thus potentially coeval with mineralized granites, or sample a mineralized granite (MY-YAD), compare

favourably with previously published geochronological data of magmatism in the range of 70-50 Ma (Barley and Khin Zaw, 2009; Sanematsu et al., 2014).

6.1.2. Collisional Stage (50-30 Ma)

Closure of the Neo-Tethys marks the transition from an accretionary to a continent-continent collisional setting and the onset of crustal thickening. Before or during this period, emplacement of Tethyan oceanic material onto the continental margins occurred. This ophiolitic material is responsible for deposits of podiform chromite, jade and nickel. Nickel laterite deposits (e.g. Tagaung Taung; Schellmann, 1989) result from later supergene reworking of ultramafics.

Ongoing orogeny and enhanced crustal thickening drove metamorphism and anatexis. This protracted metamorphic event was also responsible for the formation of the marble-hosted gemstones found at Mogok; namely ruby, sapphire and spinel (Searle et al., 2016). In Myanmar, it is possible that the amphibolite-grade metamorphism resulted in the release of scavenging fluids and the subsequent development of the orogenic Au deposits although this is subjective and is discussed below.

During this period the Eocene diorite that hosts the Shangalon Cu-Au deposit was intruded, which we suggest provides a best estimate for the porphyry-type mineralization observed here.

6.1.3. Late Collisional Stage (30-20 Ma)

Geochronology suggests a Miocene-age, period of WPA activity during this period, responsible for the development of the Monywa Cu epithermal deposit. Late-stage magmatism is associated with the

development of skarn-type deposits within the high-T marbles of the Mogok Metamorphic Belt.

6.1.4. Highly-Oblique Collisional Stage (15-0 Ma)

The continuing northwards movement of the Indian Plate drove the clockwise rotation of terranes around the syntaxis during Oligocene-Miocene times, and initiated movement on the strike-slip Sagaing Fault. Faulting is interpreted to have helped drive sandstone-hosted low-sulphidation epithermal Au mineralization, driven by circulation of auriferous hydrothermal fluids, and occurring as vein stockworks in small pull-apart basins (example of Kyaukpahto; Ye Myint Swe et al., 2004). Fig. 5C shows a schematic genesis for such seismically-pumped gold deposits.

6.2. Discussion

In Myanmar, limited zircon U-Pb geochronology has yielded the magmatic ages of granites. According to metallogenetic interpretations, these ages can inform on the age of mineralization of granite-hosted ore deposits. However, a number of mineralization styles presented here lack firm age constraints. In our model we therefore derived proposed ages of their geneses on the basis of inferred tectonic settings, and below we discuss the evidence and limitations for placing these less well-constrained deposits into our metallogenic framework.

6.2.1. Age of Magmatic-Hydrothermal Tin-Tungsten deposits

There are limited age constraints on the crystallization ages of tin-hosting granites, and even less work on constraining the actual age of mineralization. In general, tin-tungsten mineralization appears to be spatially

associated with Palaeogene S-type granites, and major deposits whose crystallization age has been constrained through zircon U-Pb geochronology include Hermyingyi (62 Ma; Barley and Khin Zaw, 2009), Mawchi (45-43 Ma; Aung Zaw Myint et al., 2016), and Yadanabon (51 Ma, our new data). We suggest that the age of mineralization of these southern Myanmar tin granites is best estimated from the magmatic crystallization ages.

6.2.2. Age of Porphyry and Epithermal Deposits

Geochronology from the WPA records at least two major epochs of magmatic activity: Late Cretaceous to Eocene and late Cenozoic. The only two definitively dated deposits are Eocene (Shangalon; MY145 age data presented here) and Miocene (Monywa) (Mitchell et al., 2011). There have been no reported ages of either porphyry-type or epithermal mineralization from the late Mesozoic despite this being the timing of the main batholith intrusions. This may be due to a lack of analyses, poor preservation potential of such high-level deposits, or simply that no mineralization occurred during this earlier magmatic event.

6.2.3. Orogenic Gold

The age and origin of the quartz-hosted gold mineralization found within the Slate Belt is not well constrained. Despite the presence of local granite intrusions, mineralization is not spatially related to these granites. Mitchell et al. (2004), in their study of Modi Taung, inferred it to be of orogenic style, linking its genesis with migrating fluids liberated during metamorphism of the Mogok Metamorphic Belt. They interpreted this metamorphism to be Jurassic in age, thus inferring this age for the mineralization, although Searle et al. (2007) have proposed a much younger Palaeogene age for peak Mogok

metamorphism. Mitchell et al. (2004), on the basis of cross-cutting evidence considered that the orogenic gold-hosting quartz veins were emplaced prior to granite magmatism. Zircon LA-ICP-MS U-Pb dating of dykes that intrude the mineralization have yielded an age of 49 ± 1 Ma (Eskine et al., 2015), providing a lower age boundary.

Globally, orogenic gold deposits are typically associated with the waning stages of orogenic compression and metamorphism. Mineralization results from the release of fluids during regional metamorphism which then migrate to higher levels in the mid-crust, and occurs in rocks of amphibolite to greenschist facies grades (Bierlein and Crowe, 2000; Goldfarb and Groves, 2015; Goldfarb et al., 2005; Groves et al., 1998). Orogenic gold deposits are found both within pre-collisional accretionary margins, and post-collisional orogenic belts. Fig. 5B shows a schematic for the genesis of Myanmar's Slate Belt Orogenic gold.

At least two major orogenic events have affected Myanmar during the Mesozoic-Cenozoic, and which could be candidates for causing widespread regional metamorphism and therefore driving the Slate Belt gold mineralization. The Indosinian Orogeny has an inferred suture zone some 100-300 km west in present day terms, and linking such a relatively distal orogenic event to the gold mineralization requires the closure of any intermediate ocean basin (e.g., Meso-Tethys) by Late Triassic times, the age of Palaeo-Tethyan suturing. If the Au mineralization were related to the closure of the Neo-Tethys, the 49 Ma age of dyke intrusion as reported by Eskine et al. (2015), does not preclude it to be related to the Eocene onset of the Himalayan Orogeny. The timing thus remains equivocal.

6.2.4. Sediment-hosted Pb-Zn sulphide deposits

Sediment-hosted deposits have a genesis related to the circulation of low-temperature brines usually in response to far-field orogenic events (Leach et al., 2005), and hosted in carbonate platforms of marginal or shelf origins. Proposed fluid drivers in such settings include a combination of thin-skin folding and thrusting and/or orogenic uplift and gravity–driven connate fluid flow.

However, no definitive ages have been published thus far to this style of mineralization in Myanmar, although their hosting Lower Palaeozoic sequences provide a maximum age bracket. One MVT-type deposit within Sibumasu has been interpreted as directly related to Cretaceous-era orogeny. Mineralization in the vicinity of Mae Sod in Thailand was interpreted to have developed in response to Cretaceous uplift and deformation on the western margin of Sibumasu (Reynolds et al., 2003). The economic-grade non-sulphide Padaeng Zn deposit was interpreted by the same authors to have formed by later supergene enrichment of local originally sulphidic MVT deposits.

7. A Tethyan Mineral System?

An orogenic system is a highly fertile regime for the provision of the geologic factors (e.g., structures, fluids, transient geodynamic trigger) that promote the generation and preservation of mineral deposits, as evidenced by the variety of deposits found associated with such settings (e.g., Cawood and Hawkesworth, 2013; Groves and Bierlein, 2007; Kerrich et al., 2005). Orogenic belts accommodate the genesis of multiple types of magmatism,

and the gestation of fluids of varying compositions through elevated P-T conditions and metamorphic dehydration reactions. Furthermore, the dynamic nature of the orogenic system gives rise to a changing lithospheric architecture with evolving conduits for metalliferous fluids, widely dispersed at low concentration, to localize in high concentrations (McCuaig and Hronsky, 2014). Mineral deposits are thus commonly clustered in geological provinces with particular areas strongly endowed in specific commodities (Arribas et al., 1995; Carlson, 1991). All these orogeny-driven metal transport processes operate on a variety of scales from continent to deposit.

At the lithospheric-scales of observation described here, the identification of discrete large-scale critical geological factors that together may have influenced the formation of mineral deposits leads to a mineral systems type approach (e.g. McCuaig et al., 2010). In Myanmar, the major discrete orogen-scale factor that governs the type and distribution of mineral deposit types in Myanmar is the evolving geodynamic setting.

The major geodynamic elements evolve over the lifetime of the Himalayan Orogen in Myanmar. Magmatism is the main driver of ore formation during the early to mid part of orogenic progression, acting both as a source of heat and potentially of metals of economic interest. The geodynamic configuration of an accretionary orogen is interpreted to strongly govern the geochemical nature and spatial distribution of resultant magmatism, with implications for metallogeny (Sillitoe, 1972). Arc-type magmatism sited immediately above the subduction zone through its potential for chalcophile-type (e.g., Cu, Au and Mo) mineral deposits shows a clear relationship to subduction-driven processes (e.g., Hedenquist and

Lowenstern, 1994). In Myanmar this magmatism leads to the development of the WPA-hosted porphyry deposits, and fertilizes the overlying epithermal processes that operate at least during the Miocene. It is possible, although speculative, that Cretaceous-era deposits developed within the WPA, but which have since been either eroded or are not yet recognized.

As this margin developed over time, the input of heat and onset of crustal thickening promoted crustal anatexis, leading to the development of melts that produced compositionally evolved crustal-melt S-type granites, most likely derived from sedimentary successions, and resulting in typically more reducing granites associated with lithophile Sn-W mineralization. After the onset of suturing in the early Eocene (ca. 50 Ma), these crustal thickening effects become increasingly dominant, driving both the generation, and the movement, of various magmatic-hydrothermal fluids. Elevated P-T regimes in the mid-crust drive widespread regional metamorphism, producing substantial volumes of low salinity aqueo-carbonic fluids through dehydration and decarbonation reactions. These fluids migrate upwards, scavenging metals, which may lead to the formation of orogenic-style gold deposits in suitable host traps. Late-stage magmatism driven through high-T metamorphism leads to the development of skarn-type deposits in appropriate hosting rocks.

During the latter stages of orogeny in Myanmar the collision becomes increasingly oblique and in some cases trans-tensional, with major strike-slip faulting emerging as the dominant geodynamic regime. Faulting promotes the movement of low-T fluids and development of epithermal gold deposits in the brittle upper crust, hydrothermal fluid movement being driven by seismic pumping. Uplift and exhumation facilitates later, supergene

alteration, leading to the development of the Ni laterite deposits (Schellmann, 1989).

7.1. Timescales of Metallogeny

Advances in the dating of geological processes have shown that many ore deposits form over a relatively short time period associated with specific geological processes. Timescales of mineral deposit genesis versus geodynamic evolution vary by 2-3 orders of magnitude (Chiaradia et al., 2014). The genesis of a deposit is effectively instantaneous within the context of a favourable geodynamic setting, with fluid flow prompted by a geodynamic trigger (e.g., suturing; magmatism; seismic activity). This effectively instantaneous nature of a mineral deposit is a reflection to some extent of the necessity to concentrate metals, widely distributed in the crust, into a small space with this focusing in space mirrored also in a focusing in time. Repeated fluid movement along a major structure may transport melts but would more likely to lead to a broad halo of low metal anomalism compared to a brief intense fluid transport event that localizes its metal anomalism. When dealing with the progression of an orogen, we can define a broad time window within which there exist conditions favourable for the formation of a mineral deposit type. Within this framework the actual timescale of deposit formation is considerably shorter.

A time-space plot is presented in Fig. 7. The age constraints from deposits discussed in this paper are presented, along with a postulated time range of potential metallogenesis, which in effect represents the timescale of favourable conditions for the deposit type formation. These are

also plotted against the varying hosting lithologies, which are also a proxy for distance from the plate margin.

From this figure we can derive two key observations. Firstly, there exist temporal overlaps of favourable conditions for the formation of a particular deposit type, permitting the genesis of differing metallotects during the same period. For example, we suggest that porphyry-hosted copper and tin-tungsten granite-hosted mineralization have the potential to develop broadly contemporaneously. Secondly, this defines an evolution of the favourable conditions, leading to a genetic sequence of deposit types over the lifetime of an evolving orogen.

More generic application of this template largely depends on the uniqueness of both fertility and favourable crustal architecture. However, both the types of deposit, and the geodynamic settings discussed here for Myanmar have been commonly documented elsewhere in the world, especially during the Mesozoic-Cenozoic eras (e.g., Bierlein et al., 2009).

8. Conclusions

We report new zircon U-Pb age data that we propose help constrain the mineralization age of several styles of ore deposits found within Myanmar. We present ages for three samples of peraluminous granites sourced from the southern tin belt (75.3 ± 7.7, 70 ± 13, and 62.3 ± 0.6 Ma), as well as an age for the hosting granite of the Yadanabon Mine (50.3 ± 0.6 Ma). All these data are interpreted as magmatic ages, and are in accord with other published ages from the Sn-W district. Together, these broadly indicate magmatism in the range 75-50 Ma, which we interpret as a reasonable age

bracket estimation for the associated Sn-W mineralization. Our age data for the Shangalon diorite (40.2 ± 0.2 Ma) we also interpret as an approximate estimate for the age of associated Cu-Au porphyry-type mineralization. The Kabaing Granite in Mogok yields a magmatic age of 16.8 ± 0.5 Ma that we interpret as providing an approximate age of mineralization of the nearby skarn-type Au-base metal sulphide deposits.

We use the framework of both existing published age data, and the new data reported here, to present a metallogenetic model for Myanmar. This model documents the progression of a single orogenic event, and the concomitant development of a variety of mineralization styles and commodities during its evolution. Within this framework we also speculate on the timing of other, poorly age-constrained deposit types. Our model places the genesis of much of Myanmar's documented mineral deposits within the context of an evolving tectonic framework involving the subduction and suturing of Neo Tethys.

Acknowledgements

We are indebted to Andrew Mitchell both for his pioneering work on, and for introducing us to, the geology and mineral deposits of Myanmar. NJG acknowledges the Oxford University Fell Fund (Ref. DGD07260) and Highland Metals Pte Ltd. for financial support. Analytical support at NIGL was funded through NIGFSC grant IP-1554-0515. U Nyunt Htay is acknowledged for the sample from Yadanabon Mine. We thank Dave Sansom for drafting figures; U Kyi Htun for assistance with field logistics; Daw Than Than Nu and

U Ne Lin for accompanying us to Mogok; Thu Htet Aung and Win Zaw for driving and navigation on various trips; U Htun Lynn Shein for general support of our Myanmar work. The NordSIM facility is operated under an agreement between the research funding agencies of Denmark, Iceland, Norway and Sweden, the Geological Survey of Finland and the Swedish Museum of Natural History, and we thank Kerstin Lindén and Lev Ilyinsky for NordSIM technical support. We thank Tony Barber and Michael Crow for insightful reviews, plus an anonymous reviewer for comments on an earlier version of this manuscript, all of which have greatly improved this work. We are grateful to Franco Pirajno for editorial handling.

References

Acharyya, S.K., 2010. Tectonic evolution of Indo-Burma range with special reference of Naga-Manipur Hills. Geol. Soc. India Mem. 75, 25–43.

Acharyya, S.K., 2007. Collisional emplacement history of the Naga-Andaman ophiolites and the position of the eastern Indian suture. J. Asian Earth Sci. 29, 229–242. doi:10.1016/j.jseaes.2006.03.003

Arribas, A., Hedenquist, J.W., Itaya, T., Okada, T., Concepcion, R. A., Garcia, J.S., 1995. Contemporaneous formation of adjacent porphyry and epithermal Cu-Au deposits over 300 ka in northern Luzon, Philippines. Geology 23, 337–340. doi:10.1130/0091-7613(1995)023<0337:CFOAPA>2.3.CO;2

Aung Zaw Myint, Khin Zaw, Myint Ye Swe., Yonezu, K., Cai, Y., Manaka, T., Watanabe, K., 2016. Geochemistry and geochronology of granites hosting the Mawchi Sn-W deposit, Myanmar: Implications for tectonic setting and granite emplacement, in: Barber, A.J., Crow, M.J., Khin Zaw, Rangin, C. (Eds.), Myanmar: Geology, Resources and Tectonics. The Geological Society, London.

Aye Ko Aung, 2012. The Palaeozoic stratigraphy of Shan Plateau, Myanmar - an up-dated version. J. Myanmar Geosci. Soc. 5, 1–73.

Barber, A.J., Crow, M.J., 2009. Structure of Sumatra and its implications for the tectonic assembly of Southeast Asia and the destruction of Paleotethys. Isl. Arc 18, 3–20.

Barber, A.J., Crow, M.J., Khin Zaw, Rangin, C., 2016. Myanmar: Geology, Resources and Tectonics. The Geological Society, London.

Barley, M.E., Groves, D.I., 1992. Supercontinent cycles and the distribution of metal deposits through time. Geology 20, 291–294. doi:10.1130/0091-7613

Barley, M.E., Khin Zaw, 2009. SHRIMP U-Pb in zircon geochronology of granitoids from Myanmar : temporal constraints on the tectonic evolution of Southeast Asia 11, 3842.

Barley, M.E., Pickard, A.L., Khin Zaw, Rak, P., Doyle, M.G., 2003. Jurassic to Miocene magmatism and metamorphism in the Mogok metamorphic belt and the India-Eurasia collision in Myanmar. Tectonics 22, 1–11. doi:10.1029/2002TC001398

Barr, S.M., Macdonald, A.S., 1991. Toward a late Paleozoic-early Mesozoic tectonic model for Thailand. Thail. J. Geosci. 1, 11–22.

Begg, G.C., Hronsky, J. A. M., Arndt, N.T., Griffin, W.L., O'Reilly, S.Y., Hayward, N., 2010. Lithospheric, cratonic, and geodynamic setting of Ni-Cu-PGE sulfide deposits. Econ. Geol. 105, 1057–1070. doi:10.2113/econgeo.105.6.1057

Bender, F., 1983. Geology of Burma. Gebriider Borntraeger, Stuttgart.

Bierlein, F.P., Crowe, D.E., 2000. Phanerozoic orogenic lode gold deposits, in: Reviews in Economic Geology v. 13. Society of Economic Geology, pp. 103–140.

Bierlein, F.P., Groves, D.I., Cawood, P.A., 2009. Metallogeny of accretionary orogens - The connection between lithospheric processes and metal endowment. Ore Geol. Rev. 36, 282–292. doi:10.1016/j.oregeorev.2009.04.002

Brunnschweiler, R.O., 1966. On the geology of the Indoburman ranges. J. Geol. Soc. Aust. 13, 137–194.

Burchfiel, B.C., Chen Zhiliang, C., 2013. Tectonics of the Southeastern Tibetan Plateau and Its Adjacent Foreland. Geol. Soc. Am. Mem. 210, 1–164. doi:10.1130/2012.1210(01)

Cao, H.-W., Zhang, S.-T., Lin, J.-Z., Zheng, L., Wu, J.-D., Li, D., 2014. Geology, geochemistry and geochronology of the Jiaojiguanliangzi Fe-polymetallic deposit, Tengchong County, Western Yunnan (China): Regional tectonic implications. J. Asian Earth Sci. 81, 142–152. doi:10.1016/j.jseaes.2013.11.002

Carlson, C. A., 1991. Spatial distribution of ore deposits. Geology 19, 111. doi:10.1130/0091-7613(1991)019<0111:SDOOD>2.3.CO;2

Cawood, P.A., Hawkesworth, C.J., 2013. Temporal relations between mineral deposits and global tectonic cycles. Geol. Soc. London, Spec. Publ. 393. doi:10.1144/sp393.1

Cawood, P.A., Johnson, M.R.W., Nemchin, A.A., 2007. Early Palaeozoic orogenesis along the Indian margin of Gondwana: Tectonic response to Gondwana assembly. Earth Planet. Sci. Lett. 255, 70–84. doi:10.1016/j.epsl.2006.12.006

Charusiri, P., Clark, A.H., Farrar, E., Archibald, D., Charusiri, B., 1993. Granite belts in Thailand: evidence from the 40Ar/39Ar geochronological and geological synthesis. J. Southeast Asian Earth Sci. 8, 127–136.

Chen, G.R., Liu, H.F., Jiang, G.W., Zheng, Q.G., Zhao, S.R., Zhang, X.G., 2004. Discovery of the Shamuluo Formation in the central segment of the Bangong-Cuo-Nujiang suture zone, Tibet. Geol. Bull. China 23, 193–194.

Chhibber, H.L., 1934. The mineral resources of Burma. Macmillan and Co., London.

Chiaradia, M., Schaltegger, U., Spikings, R., 2014. Time Scales of Mineral Systems — Advances in Understanding Over the Past Decade. Soc. Econ. Geol. Spec. Publ. 18, 37–58.

Cobbing, E.J., Mallick, D.I.J., Pitfield, P.E.J., Teoh, L.H., 1986. The granites of the Southeast Asian Tin Belt. J. Geol. Soc. London. 143, 537–550. doi:10.1144/gsjgs.143.3.0537

Cobbing, E.J., Pitfield, P.E.J., Darbyshire, D., Mallick, D.I.J., Pitfield, P.E.J., Teoh, L.H., 1992. The granites of the Southeast Asian Tin Belt. J. Geol. Soc. London. 143, 537–550. doi:10.1144/gsjgs.143.3.0537

Coggin Brown, J., 1936. India's mineral wealth: A guide to the occurrences and economics of the useful minerals of the Indian Empire. Oxford University Press.

Coggin Brown, J., 1918. The cassiterite deposits of Tavoy. Rec. Geol. Surv. India 49, 23–33.

Coggin Brown, J., Heron, A., 1923. The Geology and Ore Deposits of the Tavoy District. Mem. Geol. Surv. India 44, 167–354.

Cooper, M.A., Herbert, R., Hill, G.S., 1989. The structural evolution of Triassic intermontane basins in northeastern Thailand, in: International Symposium on Intermontane Basins: Geology and Resources. Chiang Mai, Thailand, Thailand, pp. 231–242.

Cox, R., Gaskell, J., Thomas, C., 1981. Burma: A country with major unexplored mineral potential, in: Asian Mining '81. Institution of Mining and Metallurgy, London, pp. 34–45.

Curray, J.R., 2005. Tectonics and history of the Andaman Sea region. J. Asian Earth Sci. 25, 187–232. doi:10.1016/j.jseaes.2004.09.001

Curray, J.R., Moore, D.G., Lawver, L.A., Emmel, F.J., Raitt, R.W., Henry, M., Kieckhefer, R., 1979. Tectonics of the Andaman Sea and Burma, in: Watkins, T.S., Martadet, L., Dickerson, P.W. (Eds.), Geological and Geophysical Investigations of Continental Margins. AAPG Memoir, pp. 189–198.

Eskine, T., Khin Zaw, Large, R., Makoundi, C., Knight, J., 2015. Geology and Mineralization Characteristics of the Modi Taung Orogenic Gold Deposit, Central Myanmar, in: Society of Economic Geologists Annual Meeting. Hobart, Australia.

Fan, J.-J., Li, C., Xie, C.-M., Wang, M., Chen, J.-W., 2015. Petrology and U–Pb zircon geochronology of bimodal volcanic rocks from the Maierze Group, northern Tibet: Constraints on the timing of closure of the Banggong–Nujiang Ocean. Lithos 227, 148–160. doi:10.1016/j.lithos.2015.03.021

Franz, L., Tay Thye Sun, Hänni, H.A., DeCapitani, C., Thanasuthipitak, T., Atichat, W., Sun, T.T., Hänni, H.A., Capitani, C. De, 2014. A Comparative Study of Jadeite , Omphacite and Kosmochlor Jades from Myanmar , and Suggestions for a Practical Nomenclature. J. Gemol. 2, 210–229.

Fraser, G.L., Huston, D.L., Gibson, G.M., Neumann, N.L., Maidment, D., Kositcin, N., Skirrow, R.G., Jaireth, S., Lyons, P., Carson, C., Cutten, H., Lambeck, A., 2007. Geodynamic and Metallogenic Evolution of Proterozoic Australia from 1870 - 1550 Ma: a discussion (No. 2007/16), Geoscience Australia Record.

Gardiner, N.J., Robb, L.J., Searle, M.P., 2014. The metallogenic provinces of Myanmar. Appl. Earth Sci. 123, 25–38. doi:10.1179/1743275814Y.0000000049

Gardiner, N.J., Robb, L.J., Searle, M.P., Kyi Htun, Khin Zaw, 2016. The Bawdwin Mine: A Review of its Geological Setting and Genesis, in: Barber, A.J., Crow, M.J., Khin Zaw, Rangin, C. (Eds.), Myanmar: Geology, Resources and Tectonics. The Geological Society, London.

Gardiner, N.J., Searle, M.P., Morley, C.K., Whitehouse, M.P., Spencer, C.J., Robb, L.J., 2015a. The closure of Palaeo-Tethys in Eastern Myanmar and Northern Thailand: New insights from zircon U–Pb and Hf isotope data. Gondwana Res. doi:10.1016/j.gr.2015.03.001

Gardiner, N.J., Searle, M.P., Robb, L.J., Morley, C.K., 2015b. Neo-Tethyan

Magmatism and Metallogeny in Myanmar – an Andean Analogue? J. Asian Earth Sci. doi:10.1016/j.jseaes.2015.03.015

Garnier, V., Giuliani, G., Ohnenstetter, D., Fallick, A.E., Dubessy, J., Banks, D., Vinh, H.Q., Lhomme, T., Maluski, H., Pêcher, A., Bakhsh, K.A., Long, P. Van, Trinh, P.T., Schwarz, D., 2008. Marble-hosted ruby deposits from Central and Southeast Asia: Towards a new genetic model. Ore Geol. Rev. 34, 169–191. doi:10.1016/j.oregeorev.2008.03.003

Garnier, V., Maluski, H., Giuliani, G., Ohnenstetter, D., Schwarz, D., 2006. Ar–

-Ar and U–-Pb ages of marble-hosted ruby deposits from central and southeast Asia. Can. J. Earth Sci. 43, 509–532. doi:10.1139/e06-005

Garson, M.S., Amos, B.J., Mitchell, A.H.G., 1976. The geology of the area around Neyaungga and Yengan, Southern Shan State, Burma (No. 2:70), Overseas Memoir.

Garzanti, E., Baud, A., Mascle, G., 1987. Sedimentary record of the northward flight of India and its collision with Eurasia (Ladakh Himalaya, India). Geodin. Acta 1, 297–312.

Ghose, N.C., Chatterjee, N., Fareeduddin, 2014. A Petrographic Atlas of Ophiolite, An example from the eastern India-Asia collision zone. Springer India.

Goffe, B., Rangin, C., Maluski, H., 2002. Jade and associated rocks from the jade Mines area, Northern Myanmar as record of a polyphased high pressure metamorphism, in: Himalaya - Karakoram - Tibet Workshop Meeting, Abstract: Journal of Asian Earth Sciences.

Goldfarb, R.J., Baker, T., Dube, D., Groves, D.I., Hart, C.J.R., Gosselin, P., 2005. Distribution, character and genesis of gold deposits in metamorphic terranes, in: Hedenquist, J.W., Thompson, J.F.H., Goldfarb, R.J., Richards, J.P. (Eds.), Economic Geology 100th Anniversary Volume. pp. 407–450.

Goldfarb, R.J., Groves, D.I., 2015. Orogenic gold: Common or evolving fluid and metal sources through time. Lithos 233, 2–26. doi:10.1016/j.lithos.2015.07.011

Goossens, P., 1979. The metallogenic provinces of Burma: Their definitions, geologic relationships and extension into China, India and Thailand, in: Third Regional Conference on Geology and Mineral Resources of Southeast Asia.

Green, O.R., Searle, M.P., Corfield, R.I., Corfield, R.M., 2008. Cretaceous-Tertiary Carbonate Platform Evolution and the Age of the India-Asia Collision along the Ladakh Himalaya (Northwest India). J. Geol. 116, 331–353. doi:10.1086/588831

Griffith, S., 1956. The mineral resources of Burma. Mineral. Mag. 95, 9–18.

Groves, D.I., Bierlein, F.P., 2007. Geodynamic settings of mineral deposit systems. J. Geol. Soc. London. 164, 19–30. doi:10.1144/0016-76492006-065

Groves, D.I., Goldfarb, R.J., Gebre-Mariam, M. Hagemann, S.G., Robert, F.,

1998. Orogenic gold deposits: A proposed classification in the context of their crustal distribution and relationship to other gold deposit types. Ore Geol. Rev. 13, 7–27.

Hall, R., 2012. Late Jurassic–Cenozoic reconstructions of the Indonesian region and the Indian Ocean. Tectonophysics 570-571, 1–41. doi:10.1016/j.tecto.2012.04.021

Hammarstrom, J.M., Bookstrom, A.A., Dicken, C.L., Drenth, B.J., Ludington, S., Robinson, G.R., Tjahjono Setiabudi, B., Sukserm, W., Nugroho Sunuhadi, D., Yan Sze Wah, A., Zientek, M.L., 2010. Porphyry Copper Assessment of Southeast Asia and Melanesia.

Hedenquist, J.W., Lowenstern, J.B., 1994. The role of magmas in the formation of hydrothermal ore deposits. Nature 370, 519–527. doi:10.1038/370519a0

Hobson, G.V., 1940. The Development of the mineral deposit at Mawchi as determined by geology and genesis. Trans. Min. Geol. Metall. Inst. India 36, 35–78.

Hughes, R.W., Galibert, O., Bosshart, G., Ward, F., Thet Oo, Smith, M., Tay Thye Sun, Harlow, G.E., 2000. Burmese Jade: The Inscrutable Gem. Gems Gemol. 36, 2–26.

Hutchison, C.S., 1994. Gondwana and Cathaysian blocks, palaeotethys sutures and cenozoic tectonics in South-east Asia. Geol. Rundschau 83, 388–405.

Hutchison, C.S., 1975. Ophiolite in Southeast Asia. Bull. Geol. Soc. Am. 86, 797–806. doi:10.1130/0016-7606(1975)86<797:OISA>2.0.CO;2

Hutchison, C.S., Taylor, D., 1978. Metallogenesis in SE Asia. J. Geol. Soc. London. 135, 407–428. doi:10.1144/gsjgs.135.4.0407

Iyer, L.A.N., 1953. The geology and gemstones of the Mogok Stone Tract, Burma. Geol. Soc. India Mem. 82, 100.

Kerrich, R., Goldfarb, R.J., Richards, J.P., 2005. Metallogenic Provinces in an Evolving Geodynamic Framework, in: Hedenquist, J.W., Thompson, J.F.H., Goldfarb, R.J., Richards, J.P. (Eds.), Economic Geology 100th Anniversary Volume. pp. 1097–1136.

Khin Zaw, 1990. Geological, petrogical and geochemical characteristics of granitoid rocks in Burma: with special reference to the associated WSn mineralization and their tectonic setting. J. Southeast Asian Earth Sci. 4, 293–335.

Khin Zaw, Khin Myo Thet, 1983. A note on a fluid inclusion study of tin-tungsten mineralization at Mawchi Mine, Kayah State, Burma. Econ. Geol. 78, 530–534.

Khin Zaw, Meffre, S., Lai, C.K., Burrett, C., Santosh, M., Graham, I., Manaka, T., Salam, A., Kamvong, T., Cromie, P., 2014. Tectonics and metallogeny of mainland Southeast Asia - A review and contribution. Gondwana Res. 26, 5–30. doi:10.1016/j.gr.2013.10.010

Khin Zaw, Aung Pwa, Thet Aung Zan, 1984. Lead-zinc mineralization at Theingon Mine, Bawsaing, Southern Shan State, Burma: A Mississippi

Valley-type deposit ? Bull. Geol. Soc. Malaysia 17, 283–306.

Kirkland, C.L., Daly, J.S., Whitehouse, M.J., 2008. Basement-cover relationships of the Kalak Nappe Complex, Arctic Norwegian Caledonides and constraints on Neoproterozoic terrane assembly in the North Atlantic region. Precambrian Res. 160, 245–276. doi:10.1016/j.precamres.2007.07.006

Ko Ko Myint, 1994. Mineral Belts and Epochs in Myanmar. Resour. Geol. 44, 1–3.

Leach, D., Sangster, D., Kelley, D., Large, R.R., Garven, G., Allen, C., Gutzmer, J., Walters, S.G., 2005. Sediment-hosted lead-zinc deposits: A global perspective, in: Hedenquist, J.W., Thompson, J.F.H., Goldfarb, R.J., Richards, J.P. (Eds.), Economic Geology 100th Anniversary Volume. pp. 561–608.

Lin, Y.-L., Yeh, M.-W., Lee, T.-Y., Chung, S.-L., Iizuka, Y., Charusiri, P., 2013. First evidence of the Cambrian basement in Upper Peninsula of Thailand and its implication for crustal and tectonic evolution of the Sibumasu terrane. Gondwana Res. 24, 1031–1037.

Liu, C.-Z., Chung, S.-L., Wu, F.-Y., Zhang, C., Xu, Y., Wang, J.-G., Chen, Y., Guo, S., 2016. Tethyan suturing in Southeast Asia: Zircon U-Pb and Hf-O isotopic constraints from Myanmar ophiolites. Geology G37342.1. doi:10.1130/G37342.1

Ludwig, K.R., 2004. User's manual for Isoplot, 3.16: A Geochronological Toolkit for Microsoft Excel. Berkeley Geochronology Center Special Publication, Ridge Road, Berkeley CA, USA, Berkeley, USA.

Ludwig, K.R., 1998. On the Treatment of Concordant Uranium-Lead Ages. Geochim. Cosmochim. Acta 62, 665–676. doi:10.1016/S0016-7037(98)00059-3

Maurin, C., Masson, F., Rangin, C., Than Min, Collard, P., 2010. First global positioning system results in northern Myanmar: Constant and localized slip rate along the Sagaing Fault. Geology 38, 591–594.

Maurin, T., Rangin, C., 2009. Structure and kinematics of the Indo-Burmese wedge: rapid and fast growth of the outer wedge. Tectonics 28, 1–21.

Maury, R.C., Pubellier, M., Rangin, C., Wulput, L., Cotten, J., Socquet, A., Bellon, H., Guillaud, J.-P., Hla Myo Htun, 2004. Quaternary calc-alkaline and alkaline volcanism in an hyper-oblique convergence setting, central Myanmar and western Yunnan. Bull. la Société Géologique Fr. 175, 461–472.

McCuaig, T., Hronsky, J.M.A., 2014. The Mineral System Concept : The Key to Exploration Targeting. Soc. Econ. Geol. Spec. Publ. 18, 153–175.

McCuaig, T.C., Beresford, S., Hronsky, J., 2010. Translating the mineral systems approach into an effective exploration targeting system. Ore Geol. Rev. 38, 128–138. doi:10.1016/j.oregeorev.2010.05.008

Metcalfe, I., 2013. Gondwana dispersion and Asian accretion: Tectonic and palaeogeographic evolution of eastern Tethys. J. Asian Earth Sci. 66, 1–33. doi:10.1016/j.jseaes.2012.12.020

Metcalfe, I., 2011. Palaeozoic-Mesozoic history of SE Asia, in: Hall, R., Cottam, M.A., Wilson, M.E.J. (Eds.), The SE Asian Gateway: History and Tectonics of the Australia-Asia Collision. Geological Society, London Special Publication, pp. 7–35. doi:10.1144/SP355.2

Metcalfe, I., 2006. Palaeozoic and Mesozoic tectonic evolution and palaeogeography of East Asian crustal fragments: The Korean Peninsula in context. Gondwana Res. 9, 24–46. doi:10.1016/j.gr.2005.04.002

Metcalfe, I., 2002. Permian tectonic framework and palaeogeography of SE Asia. J. Asian Earth Sci. 20, 551–566. doi:10.1016/S1367-9120(02)00022-6

Metcalfe, I., 2000. The Bentong – Raub Suture Zone. J. Asian Earth Sci. 18, 691–712.

Metcalfe, I., 1984. Stratigraphy, palaeontology and palaeogeography of the Carboniferous of Southeast Asia. Mémoires la Société Géographique Fr. 147, 107–118.

MGS, 2012. Geological Map of Myanmar. Myanmar Geosciences Society, Yangon.

Mitchell, A.H.G., 1993. Cretaceous-Cenozoic tectonic events in the western Myanmar (Burma)-Assam region. J. Geol. Soc. London. 150, 1089–1102. doi:10.1144/gsjgs.150.6.1089

Mitchell, A.H.G., 1992. Late Permian-Mesozoic events and the Mergui Group nappe in Myanmar and Thailand. J. Southeast Asian Earth Sci. 7, 165–178.

Mitchell, A.H.G., 1986. Mesozoic and Cenozoic regional tectonics and metallogenesis in Mainland SE Asia. Geo. Soc. Malaysia Bull. 20, 221–239.

Mitchell, A.H.G., 1979. Rift-, Subduction- and Collision-Related Tin Belts. Geol. Soc. Malaysia Bull. 11, 81–102.

Mitchell, A.H.G., 1977. Tectonic settings for the emplacement of Southeast Asian tin granites. Geol. Soc. Malaysia Bull. 9, 123–140.

Mitchell, A.H.G., Ausa, C.A., Deiparine, L., Tin Hlaing, Nyunt Htay, Khine, A., 2004. The Modi Taung - Nankwe gold district, Slate belt, central Myanmar: Mesothermal veins in a Mesozoic orogen. J. Asian Earth Sci. 23, 321–341. doi:10.1016/S1367-9120(03)00138-X

Mitchell, A.H.G., Chung, S.-L., Thura Oo, Lin, T.H., Hung, C.H., 2012. Zircon U-Pb ages in Myanmar: Magmatic-metamorphic events and the closure of a neo-Tethys ocean? J. Asian Earth Sci. 56, 1–23. doi:10.1016/j.jseaes.2012.04.019

Mitchell, A.H.G., Garson, M.S., 1981. Mineral Deposits and Global Tectonic Settings. Academic Press, New York.

Mitchell, A.H.G., Myint Thein Htay, 2013. The Magmatic Arc and the Slate Belt: Copper-gold and Tin-tungsten and Gold Metallotects in Myanmar. East Asia: Geology, Exploration Techniques and Mines, Bali, pp. 58–59.

Mitchell, A.H.G., McKerrow, W.S., 1975. Analogous Evolution of the Burma Orogen and the Scottish Caledonides. Bull. Geol. Soc. Am. 86, 305–315.

doi:10.1130/0016-7606(1975)86<305:AEOTBO>2.0.CO;2

Mitchell, A.H.G., Myint Thein Htay, Kyaw Min Htun, 2015. The Medial Myanmar Suture Zone and the Western Myanmar- Mogok foreland. J. Myanmar Geosci. Soc. 6, 73–88.

Mitchell, A.H.G., Myint Thein Htay, Kyaw Min Htun, Myint Naing Win, Thura Oo, Tin Hlaing, 2007. Rock relationships in the Mogok metamorphic belt, Tatkon to Mandalay, central Myanmar. J. Asian Earth Sci. 29, 891–910. doi:10.1016/j.jseaes.2006.05.009

Mitchell, A.H.G., Nyunt Htay, U., Ausa, C., Deiparine, L., Aung Khine, U., Sein Po, U., 1999. Geological Settings of Gold Districts in Myanmar. Semin. Pacrim Berli.

Mitchell, A.H.G., Win Myint, Kyi Lynn, Myint Thein Htay, Maw Oo, Thein Zaw, 2011. Geology of the High Sulfidation Copper Deposits, Monywa Mine, Myanmar. Resour. Geol. 61, 1–29. doi:10.1111/j.1751-3928.2010.00145.x

Mitra, S., Priestley, K., Bhattacharyya, A.K., Gaur, V.K., 2005. Crustal structure and earthquake focal depths beneath northeastern India and southern Tibet. Geophys. J. Int. 160, 227–248.

Morley, C.K., 2012. Late Cretaceous-Early Palaeogene tectonic development of SE Asia. Earth-Science Rev. 115, 37–75. doi:10.1016/j.earscirev.2012.08.002

Ng, S.W.P., Chung, S.-L., Robb, L.J., Searle, M.P., Ghani, A.A., Whitehouse, M.J., Oliver, G.J.H., Sone, M., Gardiner, N.J., Roselee, M.H., 2015. Petrogenesis of Malaysian granitoids in the Southeast Asian tin belt: Part 1. Geochemical and Sr-Nd isotopic characteristics. Geol. Soc. Am. Bull. 1–29. doi:10.1130/B31213.1

Otofuji, Y., Mu, C.L., Tanaka, K., Miura, D., Inokuchi, H., Kamei, R., Tamai, M., Takemoto, K., Zaman, H., Yokoyama, M., 2007. Spatial gap between Lhasa and Qiangtang blocks inferred from Middle Jurassic to Cretaceous paleomagnetic data. Earth Planet. Sci. Lett. 262, 581–593. doi:10.1016/j.epsl.2007.08.013

Pollard, P., Nakapadungrat, S., Taylor, R., 1995. The Phuket Supersuite, Southwest Thailand: Fractionated I-Type Granites Associated with Tin-Tantalum Mineralization. Econ. Geol. 90, 586–602.

Rangin, C., Maurin, T., Masson, F., 2013. Combined effects of Eurasia/Sunda oblique convergence and East-Tibetan crustal flow on the active tectonics of Burma. J. Asian Earth Sci. 76, 185–194. doi:10.1016/j.jseaes.2013.05.018

Raterman, N.S.S., Robinson, A.C.C., Cowgill, E.S.S., 2014. Structure and detrital zircon geochronology of the Domar fold-thrust belt: Evidence of pre-Cenozoic crustal thickening of the western Tibetan Plateau. Geol. Soc. Am. Spec. Pap. 507 , 89–104. doi:10.1130/2014.2507(05)

Replumaz, A., Tapponnier, P., 2003. Reconstruction of the deformed collision zone Between India and Asia by backward motion of lithospheric blocks. J. Geophys. Res. 108, 2285. doi:10.1029/2001JB000661

Reynolds, N. A., Chisnall, T.W., Kaewsang, K., Keesaneyabutr, C., Taksavasu, T., 2003. The Padaeng supergene nonsulfide zinc deposit, Mae Sod, Thailand. Econ. Geol. 98, 773–785. doi:10.2113/gsecongeo.98.4.773

Richards, J.P., 2014. Tectonic, magmatic, and metallogenic evolution of the Tethyan orogen: From subduction to collision. Ore Geol. Rev. 70, 323–345. doi:10.1016/j.oregeorev.2014.11.009

Ridd, M.F., 2016. Karen-Tenasserim Unit, in: Barber, A.J., Crow, M.J., Khin Zaw, Rangin, C. (Eds.), Myanmar: Geology, Resources and Tectonics. Geological Society, London.

Ridd, M.F., 2015. Should Sibumasu be renamed Sibuma? The case for a discrete Gondwana-derived block embracing western Myanmar, upper Peninsular Thailand and NE Sumatra. J. Geol. Soc. London. 2015–065. doi:10.1144/jgs2015-065

Ridd, M.F., 2009. The Phuket Terrane: A Late Palaeozoic rift at the margin of Sibumasu. J. Asian Earth Sci. 36, 238–251. doi:10.1016/j.jseaes.2009.06.006

Ridd, M.F., Watkinson, I., 2013. Phuket-Slate Belt terrane: tectonic evolution and strike-slip emplacement of a major terrane on the Sundaland margin of Thailand and Myanmar. Proc. Geol. Assoc. 124, 994–1010.

Robb, L.J., 2004. Introduction to Ore-Forming Processes. Blackwell, Oxford.

Sanematsu, K., Manaka, T., Khin Zaw, 2014. Geochemical and Geochronological Characteristics of Granites and Sn-W-REE Mineralization in the Thanintharyi Region, Southern Myanmar. GEOSEA XIII Proc. 19–20.

Schellmann, W., 1989. Composition and origin of lateritic nickel ore at Tagaung Taung, Burma. Miner. Depos. 24, 161–168. doi:10.1007/BF00206438

Searle, D.L., Ba Than Haq, 1964. The Mogok belt of Burma and its relationship to the Himalayan orogeny, in: Proceedings of the 22nd International Geological Conference. Delhi, pp. 132–161.

Searle, M.P., Cooper, D.J., Rex, A.J., 1988. Collision tectonics of the Ladakh-Zanskar Himalaya. Philos. Trans. R. Soc. London 326, 117–150.

Searle, M.P., Morley, C.K., 2011. Tectonics and thermal evolution of Thailand in the regional context of Southeast Asia, in: Ridd, M.F., Barber, A.J., Crow, M.J. (Eds.), The Geology of Thailand. The Geological Society, London, pp. 539–572.

Searle, M.P., Morley, C.K., Waters, D.J., Gardiner, N.J., Kyi Htun, Robb, L.J., 2016. Tectonics of the Mogok Metamorphic Belt, Myanmar (Burma) and its correlations from the East Himalayan Syntaxis to the Malay Peninsula, in: Barber, A.J., Crow, M.J., Khin Zaw, Rangin, C. (Eds.), Myanmar: Geology, Resources and Tectonics. The Geological Society, London.

Searle, M.P., Noble, S.R., Cottle, J.M., Waters, D.J., Mitchell, A.H.G., Tin Hlaing, Horstwood, M.S.A., 2007. Tectonic evolution of the Mogok metamorphic belt, Burma (Myanmar) constrained by U-Th-Pb dating of

metamorphic and magmatic rocks. Tectonics 26. doi:10.1029/2006TC002083

Sevastjanova, I., Hall, R., Rittner, M., Saw Mu Tha Lay Paw, Tin Tin Naing, Alderton, D.H., Comfort, G., 2015. Myanmar and Asia united, Australia left behind long ago. Gondwana Res. doi:10.1016/j.gr.2015.02.001

Sillitoe, R.H., 1972. Relation of Metal Provinces in Western America to Subduction of Oceanic Lithosphere. Geol. Soc. Am. Bull. 83, 813–818. doi:10.1130/0016-7606(1972)83

Socquet, A., Vigny, C., Chamot-Rooke, N., Simons, W., Rangin, C., Ambrosius, B., 2006. India and Sunda plates motion and deformation along their boundary in Myanmar determined by GPS. J. Geophys. Res. Solid Earth 111, 1–11. doi:10.1029/2005JB003877

Soe Win, U., Malar Myo Myint, 1998. Mineral Potential of Myanmar. Resour. Geol. 48, 209–218.

Sone, M., Metcalfe, I., 2008. Parallel Tethyan sutures in mainland Southeast Asia: New insights for Palaeo-Tethys closure and implications for the Indosinian orogeny. Comptes Rendus - Geosci. 340, 166–179. doi:10.1016/j.crte.2007.09.008

Spencer, C.J., Roberts, N.M.W., Cawood, P.A., Hawkesworth, C.J., Prave, A.R., Antonini, A.S.M., Horstwood, M.S.A., 2014. Intermontane basins and bimodal volcanism at the onset of the Sveconorwegian Orogeny, southern Norway. Precambrian Res. 252, 107–118. doi:10.1016/j.precamres.2014.07.008

Stacey, J.S., Kramers, J.D., 1975. Approximation of terrestrial lead isotope evolution by a two-stage model. Earth Planet. Sci. Lett. 26, 207–221. doi:10.1016/0012-821X(75)90088-6

Stephenson, D., Marshall, T.R., 1984. The petrology and mineralogy of Mt. Popa Volcano and the nature of the late-Cenozoic Burma Volcanic Arc. J. Geol. Soc. London. 141, 747–762. doi:10.1144/gsjgs.141.4.0747

Stork, A.L., Selby, N.D., Heyburn, R., Searle, M.P., 2008. Accurate Relative Earthquake Hypocenters Reveal Structure of the Burma Subduction Zone. Bull. Seismol. Soc. Am. 98, 2815–2827.

Suzuki, H., Maung Maung, Aye Ko Aung, Takai, M., 2004. Jurassic radiolarian from chert pebbles of the Eocene Pondaung Formation, central Myanmar. Neues Jahrb. fur Geol. und Palaontologie 231, 369–393.

Themelis, T., 2008. Gems & Mines Of Mogok. A&T Pub. (USA).

Tin Aung Myint, Than Than Nu, Min Aung, 2014. Precious and Base Metal Mineralization in Kwinthonze-Nweyon area, Singu and Thabeikkyin Townships, Mandalay Region, Myanmar. in: Sundaland Resources. Indonesia.

UNDP, 1996. Geology and mineral resources of Myanmar. Atlas of the Mineral Regions of the ESCAP Region (No. 12), United Nations Economic and Social Commission for Asia and the Pacific.

UNDP, 1978. Geology and exploration geochemistry of the Pinlebu-Banmauk area, Sagaing Division, Northern Burma. United Nations Geological

Survey and Exploration Project. New York.

Vigny, C., 2003. Present-day crustal deformation around Sagaing fault, Myanmar. J. Geophys. Res. 108. doi:10.1029/2002JB001999

Wang, B.-D., Wang, L.-Q., Chung, S.-L., Chen, J.-L., Yin, F.-G., Liu, H., Li, X.-B., Chen, L.-K., 2015. Evolution of the Bangong–Nujiang Tethyan ocean: Insights from the geochronology and geochemistry of mafic rocks within ophiolites. Lithos. doi:10.1016/j.lithos.2015.07.016

Wang, J.G., Wu, F.Y., Tan, X.C., Liu, C.Z., 2014. Magmatic evolution of the Western Myanmar Arc documented by U-Pb and Hf isotopes in detrital zircon. Tectonophysics 612-613, 97–105. doi:10.1016/j.tecto.2013.11.039

Wang, Y., Xing, X., Cawood, P.A., Lai, S., Xia, X., Fan, W., Liu, H., Zhang, F., 2013. Petrogenesis of early Paleozoic peraluminous granite in the Sibumasu Block of SW Yunnan and diachronous accretionary orogenesis along the northern margin of Gondwana. Lithos 182-183, 67–85. doi:10.1016/j.lithos.2013.09.010

Whitehouse, M.J., Kamber, B.S., 2005. Assigning dates to thin gneissic veins in high-grade metamorphic terranes: A cautionary tale from Akilia, southwest Greenland. J. Petrol. 46, 291–318. doi:10.1093/petrology/egh075

Whitehouse, M.J., Kamber, B.S., Moorbath, S., 1999. Age significance of U–Th–Pb zircon data from early Archaean rocks of west Greenland—a reassessment based on combined ion-microprobe and imaging studies. Chem. Geol. 160, 201–224. doi:10.1016/S0009-2541(99)00066-2

Ye Myint Swe, Lee, I.S., Than Htay, Min Aung, 2004. Gold mineralization at the Kyaukpahto mine area, northern Myanmar. Resour. Geol. 54, 197–204.

Zahirovic, S., Seton, M., Müller, R.D., 2014. The Cretaceous and Cenozoic tectonic evolution of Southeast Asia. Solid Earth 5, 227–273. doi:10.5194/se-5-227-2014

Zaw Naing Oo, Khin Zaw, 2009. Geology and mineralization characteristics of Meyon gold deposit, Mon State, Southern Myanmar, in: Proceedings of the Eleventh Regional Congress on Geology, Mineral and Energy Resources of Southeast Asia (GEOSEA). Kuala Lumpur, Malaysia, p. 32.

Zhao, S., Lai, S., Qin, J., Zhu, R.-Z., 2015. Tectono-magmatic evolution of the Gaoligong belt, southeastern margin of the Tibetan plateau: Constraints from granitic gneisses and granitoid intrusions. Gondwana Res. doi:10.1016/j.gr.2015.05.007

Zhu, D.-C., Li, S.-M., Cawood, P.A., Wang, Q., Zhao, Z.-D., Liu, S.-A., Wang, L.-Q., 2015. Assembly of the Lhasa and Qiangtang terranes in central Tibet by divergent double subduction. Lithos. doi:10.1016/j.lithos.2015.06.023

Zhu, D.-C., Zhao, Z.-D., Niu, Y., Dilek, Y., Wang, Q., Ji, W.-H., Dong, G.-C., Sui, Q.-L., Liu, Y.-S., Yuan, H.-L., Mo, X.-X., 2012. Cambrian bimodal volcanism in the Lhasa Terrane, southern Tibet: Record of an early Paleozoic Andean-type magmatic arc in the Australian proto-Tethyan margin. Chem. Geol. 328, 290–308. doi:10.1016/j.chemgeo.2011.12.024

Zi, J.W., Cawood, P.A., Fan, W.M., Wang, Y.J., Tohver, E., McCuaig, T.C., Peng, T.P., 2012. Triassic collision in the Paleo-Tethys Ocean constrained by volcanic activity in SW China. Lithos 144-145, 145–160. doi:10.1016/j.lithos.2012.04.020

Fig. 1. Geological terrane map of the Eastern Himalaya, southeast Tibet, Myanmar, Yunnan (China), and Thailand. ITPS – Indus-Tsangpo suture zone; SH – Shillong plateau; SFZ – Sagaing fault zone; TPFZ – Three Pagodas Fault zone; MPFZ – Mae Ping Fault zone; PFZ - Paung Laung Fault Zone; ST – Sibumasu; ASRR – Ailao Shan – Red River shear zone; SCT – South China terrane; EHS = Eastern Himalayan Syntaxis. WB = Western Ophiolite Belt; EB = Eastern Ophiolite Belt. After Gardiner et al. (2015b).

Fig. 2. Palaeogeographic reconstructions for the Eastern Tethys during the Late Jurassic, Early Cretaceous, Late Cretaceous and Middle Eocene. Simplified from Metcalfe (2011). S = Sibumasu; I = Indochina; SC = South China; QS = Qamdo-Simao. The Mawgyi Arc and the putative West Burma Plate (WB) are highlighted.

Fig. 3. Geological map of Myanmar, detailing the main geological provinces, and the major deposits as discussed in the text. Based on the Myanmar Geosciences Geological Map of Myanmar (MGS, 2012).

Fig. 4. Concordia diagrams showing ^{20} Pb-corrected zircon U-Pb ages, and ^{207}Pb-corrected age weighted average plots, for all samples selected for calculation of Concordia ages. All uncertainties are shown at 2 sigma.

Fig. 5. Diagrams showing the interpreted metallogenetic settings for a number of ore deposit types discussed in the text. (a) Schematic continental crust architecture during the accretionary stage with relevant magmatic-related ore

deposits; (b) Hypothetical Slate Belt Orogenic Au mineralization; prograde metamorphism of Mogok rocks at depth releases fluids that migrate into lower-grade brittle upper crust; (c) A model for the Kyaukpahto epithermal gold mine: en-echelon strike-slip fault arrays associated with extensional stresses related to movement on the Sagaing Fault. Diagrams a and c modified from Robb (2004). Diagram b modified after Groves et al. (1998) and Goldfarb and Groves (2015).

Fig. 6. Schematic tectonic evolution of Myanmar, detailing interpreted metallogenesis related to each major stage and location of major mines.

Fig. 7. Space-time chart constructed for Myanmar, showing ages of major deposits discussed in the text.

Table 1: Summary of samples, localities and age data. All age uncertainties are quoted at 2 sigma. MMM = Mogok-Mandalay-Mergui Belt; WPA = Wuntho-Popa Arc.

Table 2: Full U-Pb analyses. Errors quoted are 1σ. ^{207}Pb-corrected ages calculated as per (Ludwig, 1998).

$^{\dagger}f_{206}$%: % of common ^{206}Pb estimated from measured ^{204}Pb. Figures in parentheses are given when no common Pb correction is made (because of low ^{204}Pb levels), indicating a value calculated assuming present-day Stacey-Kramers common Pb.

Table 3: Metallotects of Myanmar discussed in the text.

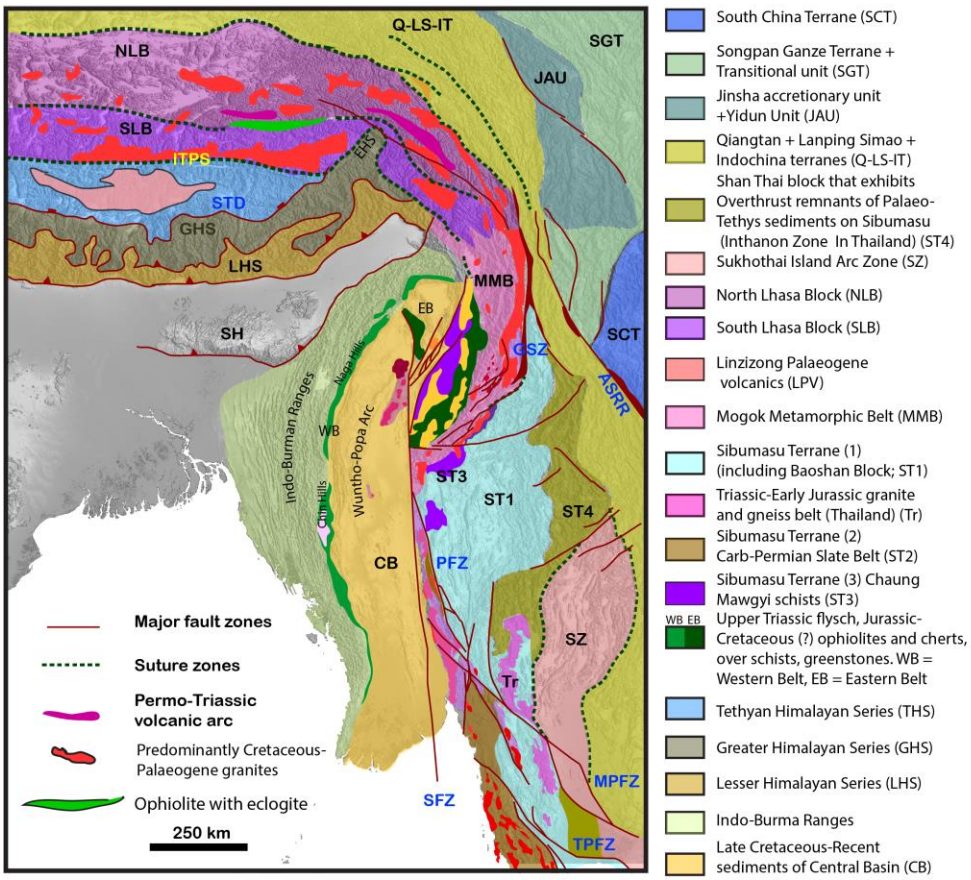

Figure 1

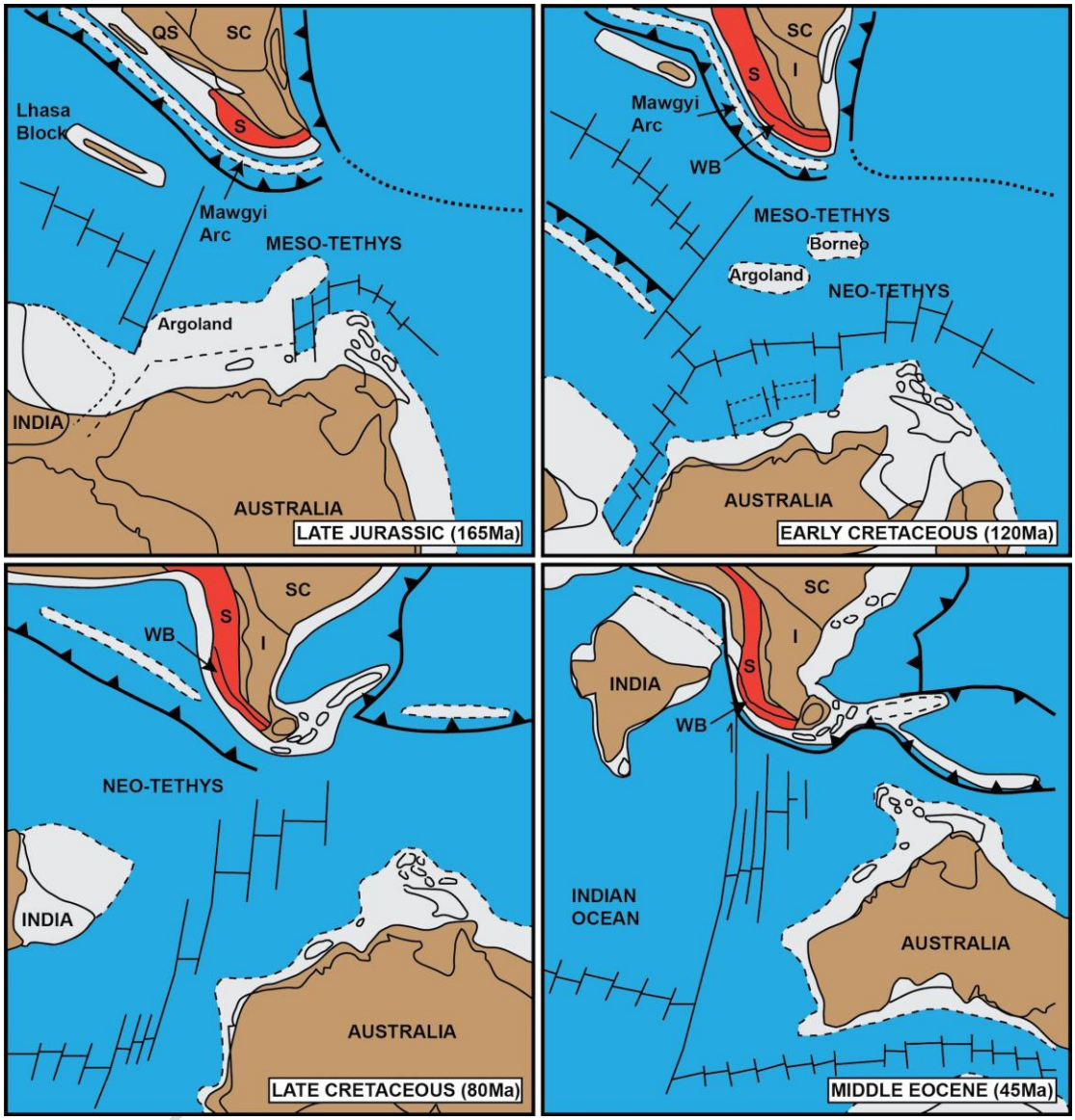

Figure 2

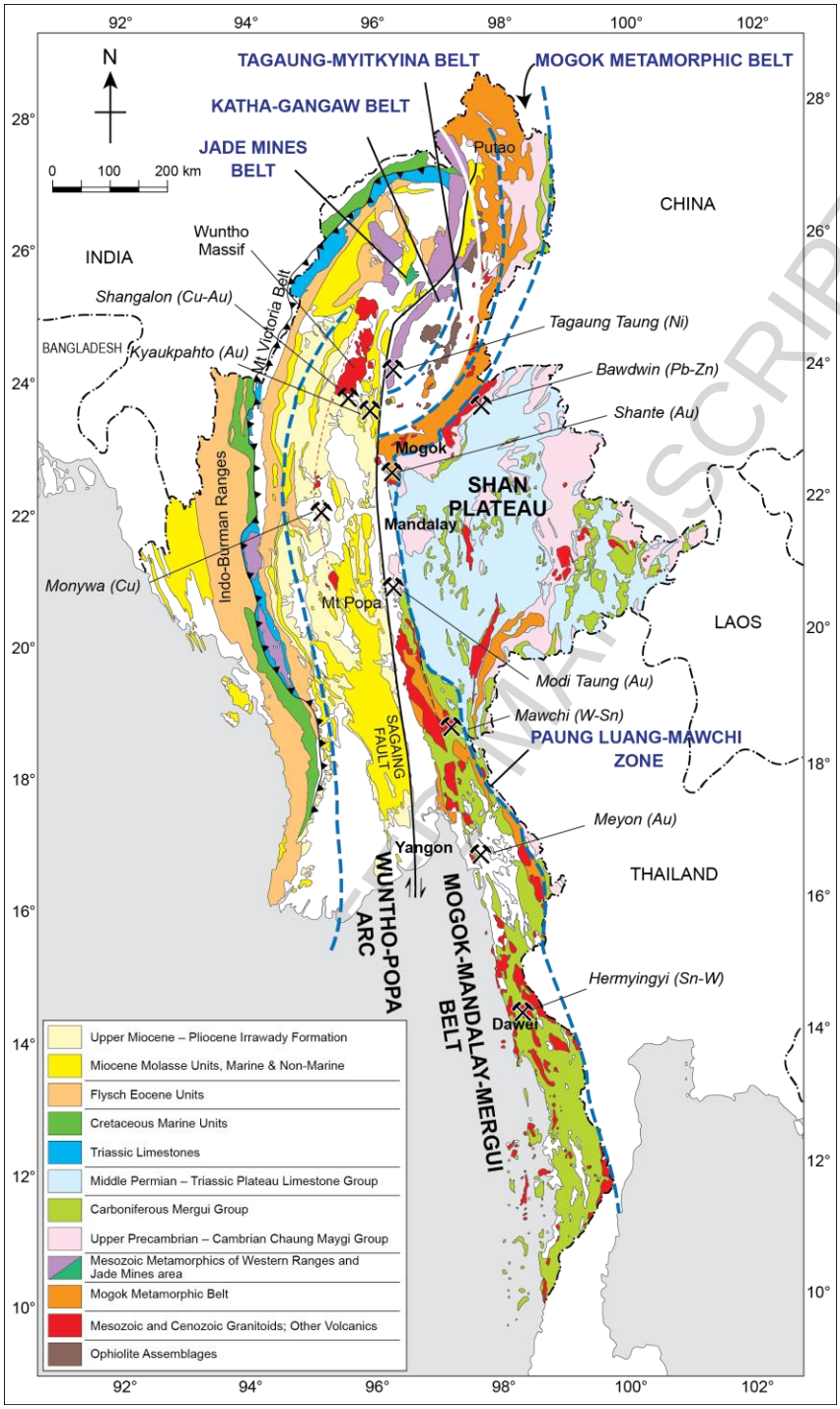

Figure 3

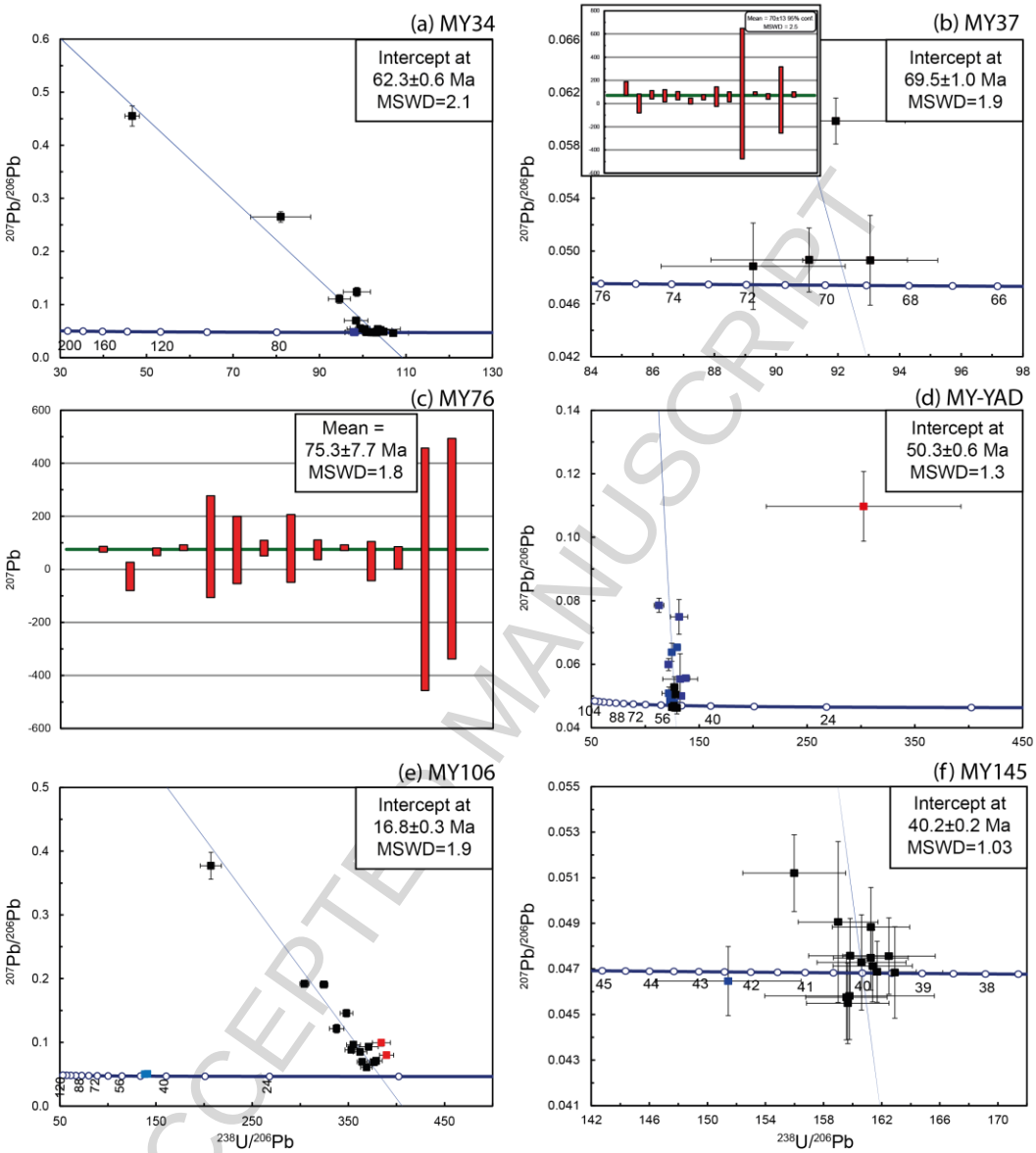

Figure 4

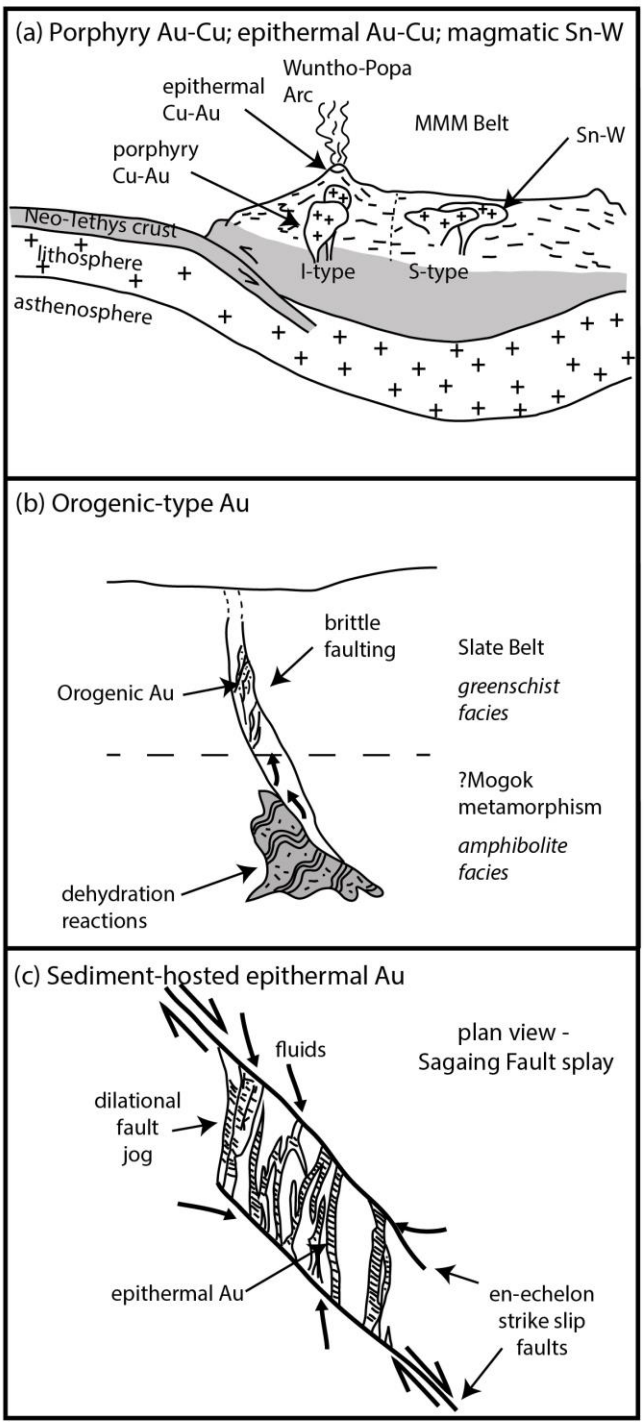

Figure 5

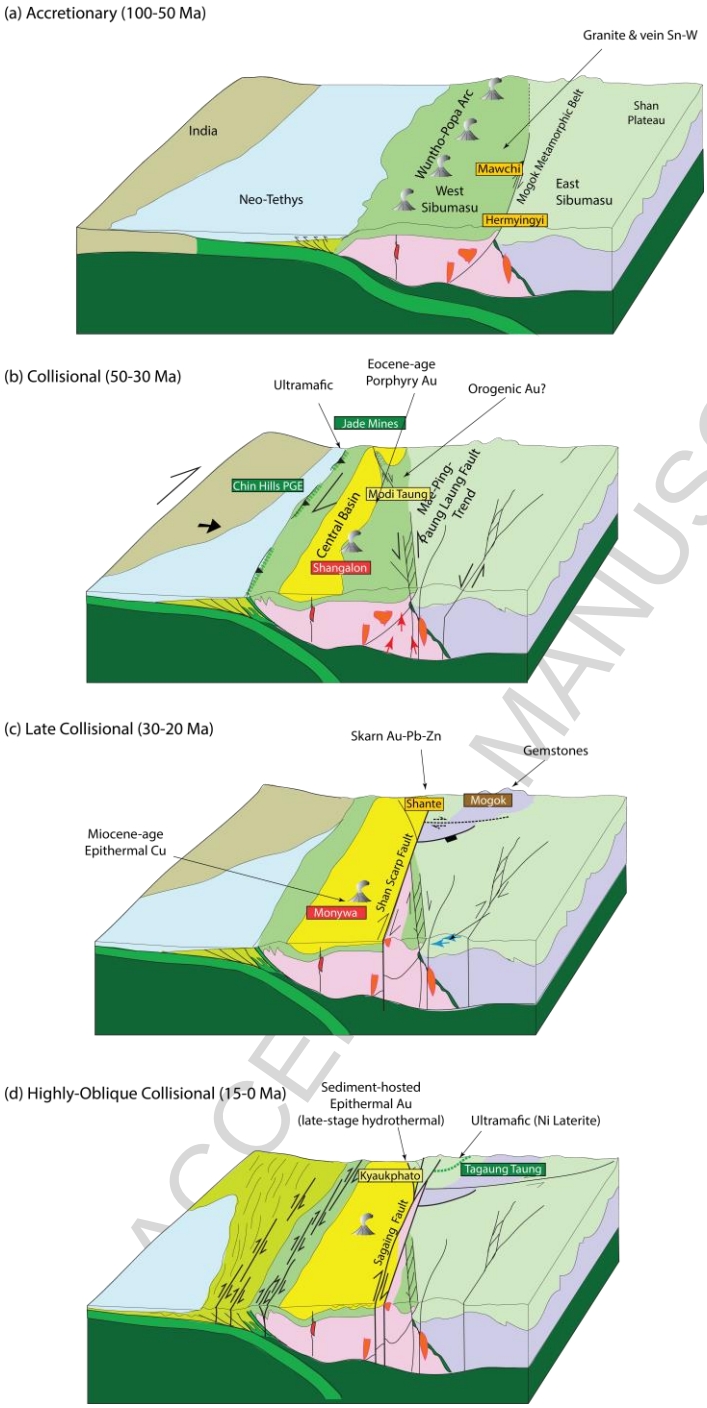

Figure 6

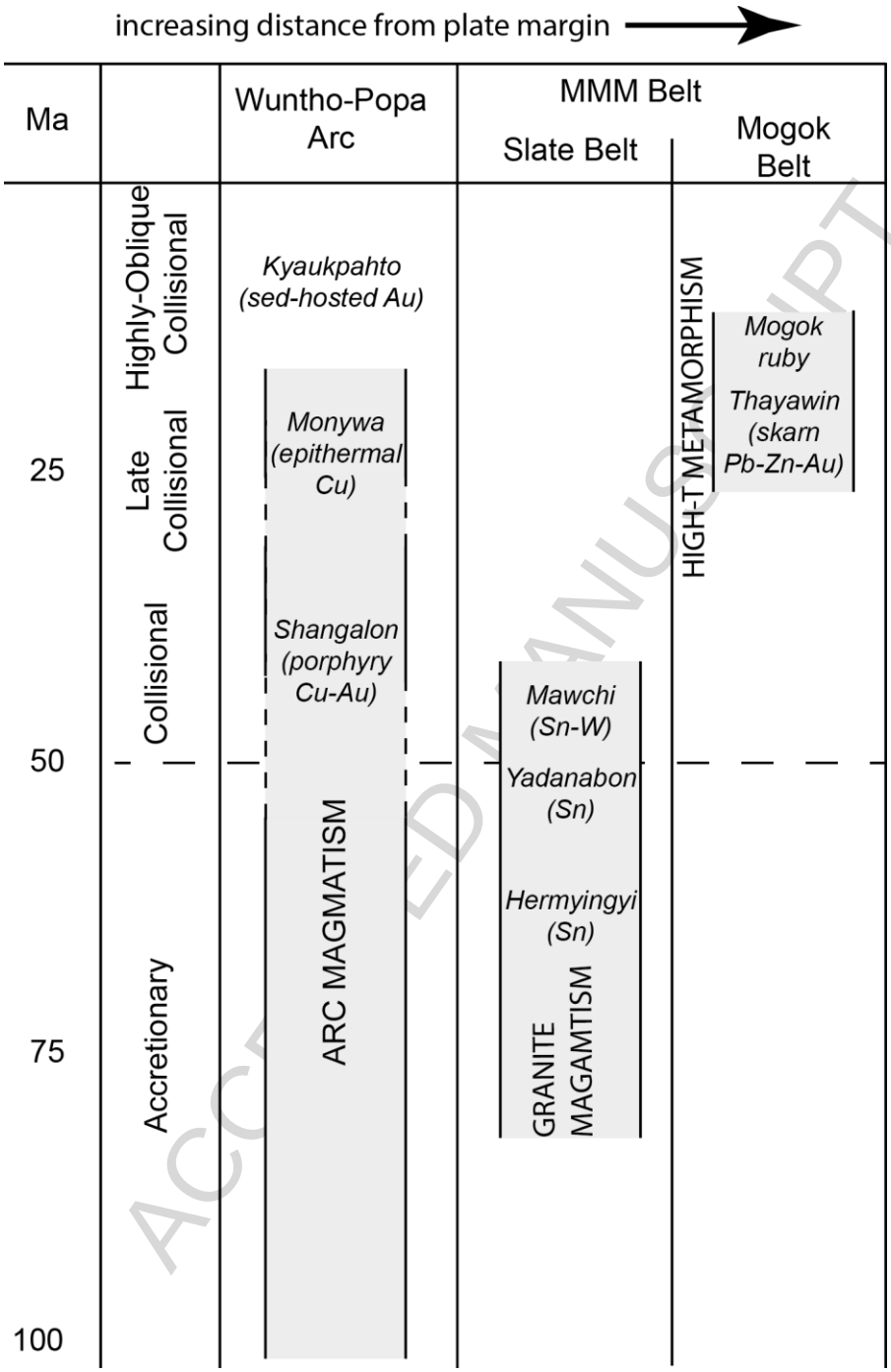

Figure 7

Table 1

ample	**Location**	**Belt**	**Location**	**ge (Ma)**
Y34	Dawei	MMM (Slate Belt)	N14.10.79 / E98.21.46	2.3±0.6
Y37	Dawei	MMM (Slate Belt)	N14.19.844 / E98.11.549	9.5±1.0
Y76	Myeik	MMM (Slate Belt)	N12,29.362 / E98.41.553	5.3±7.7
YYAD	Yadanabon Granite	MMM (Slate Belt)	N11.17.45 / E99.16.098	0.3±0.6
Y106	Kabaing Granite	MMM (Mogok)	N22.55.190 / E96.20.792	6.8±0.5
Y145	Shangalon	WPA	N23.42.025 / E95.31.277	0.0±0.2

Table 2

							204-Pb uncorrected				Ages							
Sample/ spot #	[U] ppm	[Th] ppm	[Pb] ppm	Th/U meas	$^{206}Pb/^{204}Pb$ common	f_{206}%	$^{238}U/^{206}Pb$	±σ %	$^{207}Pb/^{206}Pb$	±σ %	$^{207}Pb/^{206}Pb$	±σ	$^{207}Pb/^{235}U$	±σ	$^{206}Pb/^{238}U$	± σ	207-corr age (Ma)	± σ
MY34																		
n5107-08	223.4	206.2	2.5	0.92	18.703	11.53	98.6231	1.60	0.123733	3.40	-1063.9	686.7	38.1	10.5	57.6	0.9	58.7	1.3
n5107-20	214.8	232.2	2.7	1.08	18.703	26.63	81.0299	4.29	0.265004	1.88	526.3	425.8	70.9	15.6	58.1	2.0	57.3	3.7
n5107-06	217.8	146.2	2.6	0.67	n/a	{0.03}	107.0480	1.64	0.045965	2.19	-4.2	52.1	58.4	1.6	59.9	1.0	60.0	1.0
n5107-03	275.2	230.9	3.4	0.84	18.703	0.36	104.8302	1.35	0.048691	1.87	-8.7	61.2	59.3	1.7	61.0	0.8	61.1	0.8
n5107-14	349.0	215.5	4.1	0.62	18.703	0.61	104.1375	1.26	0.051851	1.66	52.4	63.1	61.0	1.8	61.2	0.8	61.2	0.8
n5107-05	5087.0	742.6	53.5	0.15	18.703	0.69	103.4748	2.52	0.053396	2.06	99.0	67.0	62.5	2.3	61.6	1.5	61.5	1.5
n5107-07	932.3	620.1	11.3	0.67	18.703	0.11	103.1677	1.08	0.048509	1.06	82.1	28.4	62.6	1.0	62.1	0.7	62.1	0.7
n5107-11	697.7	416.6	8.4	0.60	n/a	{0.14}	103.1510	1.04	0.047050	1.26	51.8	29.8	61.9	1.0	62.2	0.6	62.2	0.6
n5107-12	245.0	162.7	3.0	0.66	n/a	{0.10}	103.1273	1.22	0.047461	2.08	72.5	48.8	62.5	1.5	62.2	0.8	62.2	0.8
n5107-19	163.0	132.9	2.0	0.82	18.703	8.24	94.5712	1.36	0.110405	3.73	-38.8	349.5	59.8	9.4	62.2	0.8	62.4	1.1
n5107-21	143.0	74.0	1.7	0.52	n/a	{0.24}	103.0474	1.50	0.047701	3.11	84.4	72.1	62.8	2.1	62.3	0.9	62.2	0.9
n5107-10	791.3	420.9	9.4	0.53	n/a	{0.12}	102.4363	1.16	0.047658	1.43	82.3	33.5	63.1	1.1	62.6	0.7	62.6	0.7
n5107-15	1077.0	438.5	12.4	0.41	n/a	{0.03}	101.9048	0.99	0.047582	0.99	78.5	23.5	63.4	0.9	63.0	0.6	62.9	0.6
n5107-13	302.1	301.4	4.0	1.00	18.703	3.26	98.4459	1.39	0.069725	2.43	-113.8	158.5	58.7	3.9	63.0	0.9	63.3	0.9
n5107-04	689.4	324.0	8.2	0.47	n/a	{0.10}	101.3880	1.14	0.047833	1.17	91.0	27.6	64.0	1.0	63.3	0.7	63.2	0.7

n5107-01	5130.1	1598.4	58.0	0.31	18.703	0.74	100.4936	2.06	0.053516	0.69	82.9	30.1	63.9	1.5	63.4	1.3	63.3	1.3
n5107-09	408.2	367.6	5.4	0.90	n/a	{0.19}	100.8451	2.03	0.047882	1.61	93.4	37.7	64.4	1.6	63.6	1.3	63.6	1.3
n5107-16	2442.9	628.5	27.4	0.26	18.703	0.90	99.3645	1.17	0.054994	0.83	93.3	32.4	64.7	1.1	64.0	0.7	63.9	0.8
n5107-02	3355.7	1823.8	41.8	0.54	n/a	{0.02}	98.1188	1.18	0.047590	0.53	78.9	12.5	65.7	0.8	65.4	0.8	65.3	0.8
n5107-17	984.7	472.8	12.0	0.48	n/a	{0.02}	97.90 95	0.97	0.048218	1.00	110.0	23.5	66.7	0.9	65.5	0.6	65.4	0.6
MY37																		
n5102-16	361.1	279.7	4.5	0.77	18.703	3.56	91.93 44	1.22	0.059850	1.45	-1040.8	218.0	44.8	3.4	67.3	0.8	68.6	0.8
n5102-07	85.9	52.0	1.2	0.61	n/a	{0.15}	93.05 07	1.18	0.049298	3.45	162.1	78.7	71.6	2.5	68.9	0.8	68.7	0.7
n5102-05	166.8	222.3	2.7	1.33	n/a	{0.45}	91.06 92	1.75	0.049330	2.46	163.5	56.5	73.1	2.1	70.4	1.2	70.2	1.2
n5102-04	624.2	305.1	8.3	0.49	n/a	{0.14}	90.85 92	0.81	0.048629	1.25	130.0	29.1	72.3	1.0	70.6	0.6	70.5	0.5
n5102-18	119.1	101.1	1.8	0.85	n/a	{0.18}	89.25 55	1.67	0.048846	3.35	140.5	76.9	73.9	2.7	71.8	1.2	71.7	1.2
n5102-14	1692.3	742.7	22.4	0.44	18.703	0.75	87.53 77	0.89	0.051048	0.73	-50.3	32.4	69.2	1.1	72.7	0.6	72.9	0.5
n5102-15	1081.9	612.4	14.9	0.57	18.703	0.87	87.32 15	0.88	0.052929	0.90	0.0	40.7	70.7	1.3	72.8	0.6	72.9	0.5
n5102-11	1947.8	533.9	25.2	0.27	18.703	0.05	87.67 03	1.52	0.047892	0.72	75.6	17.7	73.2	1.2	73.1	1.1	73.1	1.0
n5102-13	803.6	918.8	13.1	1.14	n/a	{0.09}	86.88 65	0.84	0.047348	1.16	66.8	26.1	73.6	1.0	73.0	0.8	73.8	0.5
n5102-03	1952.0	730.0	26.2	0.37	n/a	{0.01}	86.40 28	1.31	0.047350	0.76	66.9	17.9	74.0	1.1	74.2	1.0	74.2	0.9
n5102-06	1610 4.5	884.6	202 .35	0.05	18.703	0.42	83.85 00	0.77	0.049768	0.41	21.8	12.6	74.5	0.7	76.1	0.6	76.2	0.4
n5102-19	4912.6	1042.7	65.9	0.21	18.703	0.06	82.77 73	0.86	0.047542	0.45	53.7	11.5	76.6	0.7	77.4	0.7	77.4	0.5
n5102-09	9795.4	1713.1	132.3	0.17	18.703	2.14	79.75 30	1.14	0.064097	0.95	59.6	41.9	78.0	1.6	78.6	0.9	78.7	0.8
n5102-	1680.	930.3	24.	0.5	18.703	0.11	81.25	0.8	0.048	0.7	57.1	21.	78.	0.9	78.	0.	78.8	0.

10	7		8	5			06	4	028	8		2	1		8	7		5
n5102-01	2556.1	536.2	36.4	0.21	18.703	1.76	77.2733	3.49	0.0617	7.13	85.8	281.6	81.66	10.6	81.4	2.8	81.48	2.8
n5102-17	1774 0.7	2701.9	248 .45	0.15	18.703	0.03	77.96 26	0.78	0.048 008	0.24	86.9	6.1	82. 3	0.7	82. 1	0. 6	82.1	0. 5
n5102-12	9157. 1	2668. 9	133 .2	0.29	18.703	0.14	77.72 38	1.23	0.048 318	0.33	60.6	12. 1	81. 6	1.0	82. 3	1. 0	82.3	0. 9
n5102-08	3148. 5	1871. 3	49. 7	0.59	18.703	0.87	76.71 02	1.39	0.053 465	3.80	30.0	143 .2	81. 0	5.0	82. 8	1. 1	82.9	1. 1
n5102-02	3143 1.2	5336. 9	446 .0	0.17	18.703	0.24	76.81 44	3.53	0.049 469	0.38	77.1	11. 2	83. 0	2.8	83. 2	2. 9	83.2	2. 9
MY76																		
n5324_01	2063 5.5	2155. 3	330 .9	0.10	18.703	0.10	67.15 08	0.95	0.048 293	0.20	75.4	5.3	94. 4	0.9	95. 2	0. 9	95.2	0. 9
n5324_02	1002 4.1	1321. 5	185 .7	0.13	18.703	0.82	57.27 19	1.08	0.052 002	0.54	-27.2	26. 8	104 .8	1.5	110 .7	1. 2	111.1	1. 2
n5324_03	1749 0.7	2302. 0	279 .6	0.13	18.703	0.04	67.91 24	0.93	0.047 619	0.30	65.6	7.2	93. 1	0.9	94. 2	0. 9	94.3	0. 9
n5324_04	1853 0.6	3763. 2	327 .4	0.20	18.703	0.06	63.77 86	4.33	0.048 088	0.21	81.1	5.4	99. 5	4.1	100 .2	4. 3	100.3	4. 3
n5324_05	1258 2.0	4233. 3	223 .6	0.34	18.703	2.62	66.06 52	1.42	0.068 328	1.82	84.9	95. 9	94. 0	4.0	94. 3	1. 4	94.4	1. 4
n5324_06	1499 9.1	3481. 2	232 .0	0.23	18.703	1.99	69.40 45	0.99	0.063 124	1.37	72.3	63. 5	89. 7	2.5	90. 4	0. 9	90.4	0. 9
n5324_08	2108 1.2	2119. 8	346 .7	0.16	18.703	0.87	64.83 71	0.86	0.054 458	0.35	79.7	14. 9	97. 1	1.0	97. 8	0. 8	97.9	0. 8
n5324_09	3578 0.0	3635. 1	632 .8	0.17	18.703	1.36	59.99 82	1.91	0.058 314	1.54	78.9	63. 9	104 .0	3.3	105 .1	2. 0	105.2	2. 0
n5324_10	1912 2.8	1968. 8	295 .2	0.15	18.703	0.49	69.42 12	0.95	0.051 299	0.48	73.2	18. 6	91. 1	1.1	91. 8	0. 9	91.8	0. 9
n5324_11	2269 8.2	3203. 1	377 .4	0.14	18.703	0.15	65.25 39	0.94	0.048 788	0.18	81.2	5.3	97. 2	0.9	97. 9	0. 9	97.9	0. 9
n5324_12	1100. 1	1098. 9	16. 6	1.00	18.703	0.52	89.21 29	0.96	0.050 737	0.90	30.3	36. 9	70. 3	1.2	71. 5	0. 7	71.6	0. 7
n5324_13	1206. 6	391.5	15. 8	0.32	n/a	{0.05}	87.83 81	0.96	0.046 881	0.88	43.2	20. 9	72. 1	0.9	73. 0	0. 7	73.0	0. 7
n5324_14	1105 7.2	1123. 2	163 .9	0.10	18.703	6.79	67.94 71	0.99	0.099 810	2.77	0.0	228 .6	85. 0	8.1	87. 8	0. 8	88.0	1. 2
n5324_15	4659.	1485.	53.	0.36	18.703	8.44	91.81	1.06	0.114	2.66	77.3	207	64.	5.9	64.	0.	63.9	1.

5	9	3	4	2			72	4	092	0		.7	3		0	7		0
MY-YAD																		
n5105-				0.8		{0.04	128.0	1.3	0.050	2.7	214.	61.	53.		50.	0.		0.
16	189.8	162.6	2.0	6	n/a	}	439	7	415	2	2	8	7	1.6	1	7	49.9	7
n5105-				0.5		{0.10	129.3	1.0	0.046	2.0		60.	48.		49.	0.		0.
12	450.2	247.8	4.3	5	n/a	}	785	5	261	6	0.0	0	9	1.1	6	5	49.7	5
n5105-				1.3			127.0	1.3	0.052	3.1		100	49.		50.	0.		0.
06	578.0	769.6	6.6	3	18.703	0.80	867	3	812	0	23.1	.3	6	2.2	1	7	50.2	7
n5105-				0.9		{0.04	126.6	1.8	0.046	1.8		43.	50.		50.	0.		0.
15	610.6	554.3	6.5	1	n/a	}	043	1	935	6	45.9	8	6	1.3	7	9	50.7	9
n5105-	1033.			0.4		{0.08	124.9	1.1	0.046	1.1		27.	50.		51.	0.		0.
01	0	501.2	9.9	9	n/a	}	698	9	434	5	20.2	3	7	0.8	4	6	51.4	6
n5105-	1752.		16.	0.5		{0.05	126.9	0.9	0.047	0.9		22.	51.		50.	0.		0.
09	7	900.2	7	1	n/a	}	569	9	852	7	91.9	9	4	0.7	6	5	50.5	5
n5105-	2164.	1198.	21.	0.5			121.9	2.6	0.050	1.9		64.	52.		52.	1.		1.
10	9	1	6	5	18.703	0.43	718	2	837	3	71.6	3	8	2.0	4	4	52.4	4
n5105-	2365.	1015.	22.	0.4			123.1	1.0	0.048	0.7		11.	50.		52.	0.		0.
07	3	4	5	3	18.703	0.33	167	2	458	9	-11.7	7	6	0.7	0	5	52.1	5
n5105-	2530.		21.	0.3			129.4	1.2	0.065	0.7		68.	47.		48.	0.		0.
11	0	789.5	8	1	18.703	2.42	870	7	319	7	0.0	1	6	1.3	4	6	48.4	6
n5105-	2707.	1321.	25.	0.4			124.7	1.3	0.063	2.2	108.	86.	51.		50.	0.		0.
13	4	4	4	9	18.703	1.98	193	2	782	5	3	4	7	2.0	5	7	50.4	7
n5105-	2822.	1184.	26.	0.4			124.4	1.1	0.048	0.7			50.		51.	0.		0.
08	8	0	7	2	18.703	0.28	541	4	156	2	-6.6	6.6	2	0.7	4	6	51.5	6
n5105-	4181.	1554.	40.	0.3			112.7	2.0	0.078	1.4		74.	54.		54.	1.		1.
14	1	2	4	7	18.703	3.97	626	0	560	2	63.0	0	9	2.0	7	1	54.7	1
n5105-	5345.		44.	0.1			132.4	6.1	0.055	7.2	118.	246	49.		48.	2.		2.
04	2	931.1	0	7	18.703	0.88	360	0	325	0	6	.3	5	6.2	1	9	48.0	9
n5105-	5347.	3652.	51.	0.6			121.5	1.2	0.059	1.5		89.	49.		51.	0.		0.
18	4	3	8	8	18.703	1.85	892	2	910	7	-39.8	2	9	1.9	8	6	51.9	6
n5105-	6501.	1884.	53.	0.2			137.6	1.3	0.055	0.4		20.	46.		46.	0.		0.
05	5	8	2	9	18.703	1.06	001	3	599	3	61.0	9	5	0.7	2	6	46.2	6
n5105-	1126	1482.	91.	0.1			133.4	1.1	0.049	0.3		16.	47.		47.	0.		0.
17	4.6	9	1	3	18.703	0.40	897	6	976	7	40.6	7	8	0.6	9	6	47.9	6
n5105-	6856	1185	552	0.1			131.4	3.0	0.074	3.6	142.	175	49.		47.	1.		1.
03	5.8	8.4	.0	7	18.703	3.31	644	6	920	4	2	.4	1	4.1	2	4	47.1	5
n5105-	9254	1561	305	0.1			302.5	14.	0.109	5.0	522.	271	24.		19.	2.		2.
02	7.9	7.1	.8	7	18.703	6.67	178	92	715	0	5	.2	7	4.9	9	9	19.6	9
MY106																		

MY106_01	37.4	34.5	0.1	0.92	18.674	233.93	337.7940	2.23	0.121484	5.64	1978.1	100.5	49.1	5.8	19.1	0.8	17.2	0.4
MY106_02	44.5	43.2	0.1	0.97	18.676	63.57	362.1392	2.00	0.085086	5.05	1317.5	97.9	32.4	3.5	17.8	0.7	16.9	0.4
MY106_03	165.3	58.1	0.5	0.35	18.673	16.89	324.5968	1.28	0.190565	1.99	2747.0	32.7	79.0	3.6	19.8	0.5	16.2	0.2
MY106_04	31.8	30.6	0.1	0.96	18.678	275.24	384.3062	2.44	0.099404	5.68	1612.9	105.8	35.6	4.3	16.8	0.8	15.6	0.4
MY106_05	46.5	74.2	0.1	1.60	18.675	143.15	348.0442	1.87	0.145643	4.06	2295.4	69.8	56.9	4.9	18.5	0.7	16.2	0.3
MY106_06	44.8	49.1	0.1	1.10	18.678	33.75	389.7663	1.90	0.079911	4.08	1194.8	80.6	28.3	2.5	16.5	0.6	15.8	0.3
MY106_07	75.6	66.0	0.2	0.87	18.677	105.94	368.8773	1.62	0.060841	3.66	633.6	78.8	22.8	1.8	17.5	0.6	17.1	0.3
MY106_08	292.6	101.4	2.2	0.35	18.634	6.98	141.2227	1.31	0.050416	1.19	214.2	27.6	48.8	1.7	45.5	1.2	45.3	0.6
MY106_09	285.0	104.1	2.1	0.37	18.633	19.37	138.3688	1.30	0.049947	1.05	192.5	24.4	49.3	1.6	46.4	1.2	46.2	0.6
MY106_10	38.8	41.4	0.2	1.07	18.656	82.80	207.1011	5.30	0.377076	5.60	3820.1	84.6	227.3	30.9	31.1	3.3	18.1	1.3
MY106_11	56.0	38.7	0.2	0.69	18.676	107.93	355.3378	2.01	0.096183	4.86	1551.4	91.3	37.2	3.8	18.1	0.7	17.0	0.4
MY106_12	55.9	39.9	0.2	0.71	18.678	89.80	378.8904	1.64	0.071035	3.37	958.4	68.9	25.9	1.9	17.0	0.6	16.5	0.3
MY106_13	36.5	45.1	0.1	1.24	18.677	167.70	371.0562	2.67	0.092984	5.08	1487.6	96.3	34.5	3.9	17.3	0.9	16.3	0.4
MY106_14	30.6	35.6	0.1	1.17	18.676	193.37	353.0892	1.86	0.088196	4.37	1386.8	83.8	34.4	3.2	18.2	0.7	17.3	0.3
MY106_15	53.8	52.4	0.1	0.97	18.677	51.01	364.5232	1.44	0.069388	4.51	910.3	92.9	26.3	2.5	17.7	0.5	17.1	0.3
MY106_16	58.3	74.1	0.2	1.27	18.671	114.84	304.2942	1.54	0.191894	2.79	2758.5	45.8	84.6	5.2	21.2	0.6	17.3	0.3
MY106_17	66.2	66.5	0.2	1.00	18.677	51.99	376.7337	1.40	0.068647	3.42	888.1	70.6	25.2	1.8	17.1	0.5	16.6	0.2
MY145																		

n5329_		1564.		3.2		{0.30	159.7	1.8	0.045	2.0		49.	39.		40.	0.		0.
@1	482.4	2	6.4	4	6301	}	840	3	815	9	-12.1	8	4	1.1	2	7	40.3	7
n5329_		1252.		1.6			155.9	1.1	0.051	1.6		53.	39.		40.	0.		0.
@02	782.8	0	7.6	0	2396	0.78	761	3	205	5	-53.8	8	3	1.2	9	5	41.0	5
n5329_		1211.		2.7		{0.16	160.6	0.9	0.047	2.2		51.	40.		40.	0.		0.
@04	437.8	9	5.3	7	11392	}	102	5	284	1	63.6	9	4	1.0	0	4	40.0	4
											-							
n5329_		2334.		3.1			159.5	0.8	0.045	2.0	148.	63.	37.		40.	0.		0.
@05	735.2	3	9.4	8	6110	0.31	695	8	755	4	6	3	2	1.0	1	4	40.3	4
n5329_		2498.		3.6		{0.05	162.4	0.9	0.047	1.7		41.	40.		39.	0.		0.
@06	687.2	5	9.4	4	36296	}	949	8	564	7	77.7	4	2	0.8	5	4	39.5	4
n5329_		1823.	13.	1.9			161.2	0.8	0.047	1.4		48.	38.		39.	0.		0.
@07	946.1	0	9	3	5913	0.32	492	0	487	9	-56.4	7	2	0.8	7	3	39.8	3
											-							
n5329_		2606.	12.	3.3			151.4	1.6	0.046	1.6	272.	73.	37.		42.	0.		0.
@08	773.9	2	6	7	2847	0.66	353	6	467	3	2	1	2	1.2	2	7	42.5	7
n5329_		2355.		3.4			159.8	0.9	0.047	1.7		57.	38.		40.	0.		0.
@09	683.6	1	9.1	5	5452	0.34	285	0	577	2	-63.0	1	4	1.0	1	4	40.2	4
n5329_		2509.		3.4			161.2	0.8	0.048	1.7		52.	39.		39.	0.		0.
@10	730.4	0	9.7	4	6460	0.29	560	3	836	8	26.3	5	5	0.9	7	3	39.8	3
n5329_		1919.		3.3		{0.06	159.6	0.8	0.045	1.9		29.	39.		40.	0.		0.
@11	574.7	9	7.7	4	30798	}	658	9	496	5	-29.0	0	1	0.8	2	4	40.3	4
											-							
n5329_		2820.	10.	3.4			161.3	0.8	0.047	1.6	150.	66.	36.		39.	0.		0.
@12	825.3	5	8	2	3868	0.48	768	5	128	7	5	9	7	1.0	6	3	39.8	3
											-							
n5329_		2397.		4.1			158.9	0.8	0.049	3.6	120.	113	37.		40.	0.		0.
@13	572.4	9	8.5	9	2828	0.66	987	6	058	0	7	.9	6	1.8	2	3	40.3	4
n5329_	1122.	6275.	19.	5.5			161.6	0.8	0.046	1.4		39.	38.		39.	0.		0.
@14	4	4	4	9	9345	0.20	858	3	874	2	-39.9	9	4	0.7	7	3	39.7	3
											-							
n5329_		1190.		2.3			162.9	1.0	0.046	2.1	101.	69.	37.		39.	0.		0.
@15	513.6	5	5.5	2	5541	0.34	058	1	843	4	1	3	1	1.1	3	4	39.4	4

Table 3

Deposit Type	Commodity	Deposit	Notes	Age
1.Magmatic-hydrothermal granite & pegmatite-hosted	**Sn-W**	Mawchi	wolframite + cassiterite	45-43 Ma[1]
	Sn	Hermyingyi		62 Ma[2]
	Sn	Yadanabon		50 Ma[3]
2. Skarn	**Au**	Thayawin	marble-hosted native Au and Pb-Zn sulphides	17 Ma[3]
	Au (+Pb+Zn)	Kwinthonze		
3. Porphyry	**Cu+Au**	Shangalon		40 Ma[3]
4. Epithermal	**Cu**	Monywa	high sulphidation	Miocene[4]
5. Ultramafic	**Ni**	Tagaung Taung	supergene laterite	
	PGE	Chin Hills	podiform Cr	
	jade	Hpakant Jade B	high-P metamorphism	?Eocene[5]
6. Orogenic Au	**Au+Ag**	Meyon	structurally controlled	Cretaceous-Palaeogene[6]
	Au	Modi Taung	quartz vein hosted	
7. Sediment-hosted Pb-Zn	**Pb+Zn**	Yadana Theingi	Ordovician carbonate hosted	
	Pb+Zn (+Cu)	Thaingon		
8. Gemstones	**ruby/sapphire**	Mogok stone tra	high-T metamorphism	Eocene-Oligocene[7]
9.Sediment-hosted epithermal Au	**Au**	Kyaukpahto	sandstone-hosted	<Eocene[8]

[1]Aung Zaw Myint et al. (2016). [2]Mitchell et al. (2012). [3]This study, [4]Mitchell et al. (2011). [5]Searle et al. (2016). [6]Zaw Naing Oo and Khin Zaw (2009). [7]Searle et al. (2007). [8]Ye Myint Swe et al. (2004)

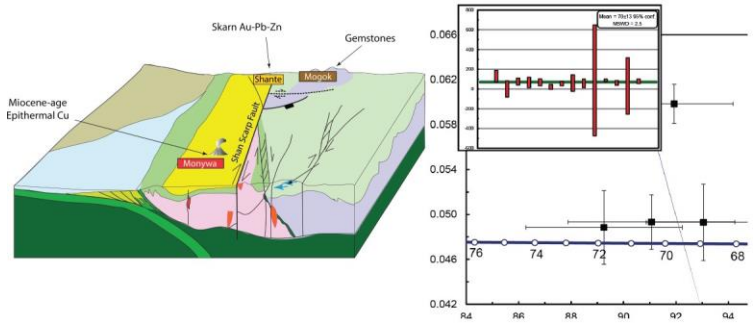

Graphical Abstract

Highlights

- New zircon U-Pb ages from several localities in Myanmar are reported
- We detail nine major metallogenic styles in Myanmar
- We outline a tectonic model for Myanmar during the Cenozoic
- We discuss a metallogenic model to place many of Myanmar's deposits in this setting
- We make observations regarding metallogenic progression during orogeny